

JAERI-M  
92-023

DEVELOPMENT OF A GLOW CURVE MEASURING  
SYSTEM OF TLDS AND ITS APPLICATIONS

March 1992

Nobuteru NARIYAMA\*, Shun-ichi TANAKA  
Michio YOSHIZAWA, Hideo HIRAYAMA,\*\* Shuichi BAN\*\*  
Hiroshi NAKASHIMA, Yoshihito NAMITO\*\*  
and Yoshihiro NAKANE

JAERI-Mレポートは、日本原子力研究所が不定期に公刊している研究報告書です。

入手の問合わせは、日本原子力研究所技術情報部情報資料課（〒319-11茨城県那珂郡東海村）あて、お申しこしてください。なお、このほかに財団法人原子力弘済会資料センター（〒319-11茨城県那珂郡東海村日本原子力研究所内）で複写による実費頒布をおこなっております。

JAERI-M reports are issued irregularly.

Inquiries about availability of the reports should be addressed to Information Division, Department of Technical Information, Japan Atomic Energy Research Institute, Tokai-mura, Naka-gun, Ibaraki-ken 319-11, Japan.

© Japan Atomic Energy Research Institute, 1992

---

編集兼発行 日本原子力研究所  
印刷 日立高速印刷株式会社

Development of a Glow Curve Measuring System of  
TLDs and its Applications

Nobuteru NARIYAMA<sup>\*</sup>, Shun-ichi TANAKA, Michio YOSHIZAWA  
Hideo HIRAYAMA<sup>\*\*</sup>, Shuichi BAN<sup>\*\*</sup>, Hiroshi NAKASHIMA  
Yoshihito NAMITO<sup>\*\*</sup> and Yoshihiro NAKANE

Department of Reactor Engineering  
Tokai Research Establishment  
Japan Atomic Energy Research Institute  
Tokai-mura, Naka-gun, Ibaraki-ken

(Received January 31, 1992)

A glow curve measurement apparatus of TLDs with a constant heating rate and a wide measurable range has been developed to study the characteristics of TLDs and to apply them to synchrotron radiation dosimetry. The heating rates of 0.5, 1, 2, 3, and 5 °C/s are controlled within an accuracy of  $\pm 2\%$  from room temperature up to 450 °C and the TL output corresponding to the photomultiplier current from 0.01 nA to 100  $\mu$ A can be measured as digital values per every 1 msec through a current digitizer, in which the linearity of the current digitizer is guaranteed with an accuracy less than 0.1 %.

The glow curve and the dose response of LiF, Li<sub>2</sub>B<sub>4</sub>O<sub>7</sub>(Mn), and Li<sub>2</sub>B<sub>4</sub>O<sub>7</sub>(Cu) TLDs have been measured for <sup>60</sup>Co gamma-rays and synchrotron radiations of 10 to 40 keV up to a couple of 10<sup>3</sup> Gy using the present system. Apparent differences among the glow curves and the dose responses have been observed with respect to the photon energy and the exposure. Consequently, the high performance of the present measuring system has been demonstrated.

Keywords : TLD Reader, TLD, LiF, Li<sub>2</sub>B<sub>4</sub>O<sub>7</sub>, Glow Curve,  
Supralinearity, Synchrotron Radiation, <sup>60</sup>Co.

---

\* Ship Research Institute

\*\* National Laboratory for High Energy Physics

TLD グローカーブ測定システムの開発とその応用

日本原子力研究所東海研究所原子炉工学部

成山 展照\*・田中 俊一・吉澤 道夫・平山 英夫\*\*  
伴 秀一\*\*・中島 宏・波戸 芳人\*\*・中根 佳弘

(1992年1月31日受理)

熱ルミネッセンス線量計 (TLD) の基本的特性を調べシンクロトロン放射光用線量計として応用するため、直線加熱特性と広測定領域をもつ TLD グローカーブ測定器を開発した。本測定器は 0.5, 1, 2, 3, 5°C/s の加熱速度を室温から 450°C まで ±2% の直線性で制御し、0.01 nA から 100 μA の光電子増倍電流に対する TL 出力を電流デジタイザーで 1 m 秒毎にデジタル化して測定できる。電流デジタイザーの直線性は 0.1% 以下の精度で保証されている。

本システムを用いて  $^{60}\text{Co}$   $\gamma$  線と 10 keV から 40 keV のシンクロトロン放射光に対する LiF,  $\text{Li}_2\text{B}_4\text{O}_7$  (Mn),  $\text{Li}_2\text{B}_4\text{O}_7$  (Cu) TLD のグローカーブと線量特性を数千 Gy までの線量において測定した。光子エネルギーと線量に関するグローカーブ間及び線量特性間の明らかな相違が観察され、本測定システムの優れた性能が示された。

---

東海研究所：〒319-11 茨城県那珂郡東海村白方字白根2-4

\* 船舶技術研究所

\*\* 高エネルギー物理学研究所

Contents

1. Introduction .....	1
2. Glow Curve Measuring System of TLDs .....	1
3. Application to TLD Material Research .....	3
3.1 <sup>60</sup> Co Gamma-ray Experiments .....	3
3.2 Experiments with Synchrotron Radiations .....	4
4. Conclusion .....	6
Acknowledgements .....	6
References .....	7

目 次

1. 序 言 .....	1
2. TLD グローカーブ測定システム .....	1
3. TLD 研究への応用 .....	3
3.1 <sup>60</sup> Co γ線照射実験 .....	3
3.2 シンクロトロン放射光照射実験 .....	4
4. まとめ .....	6
謝 辞 .....	6
参考文献 .....	7

## 1. Introduction

Thermoluminescence dosimeters (TLDs) have been used for personal dosimetry of gamma-rays above several tenth keV, and it also has been expected to be a promising one for synchrotron radiations which are very intense X-rays having energies less than several tenth keV, because TLDs have great flexibility in the choice of materials and size. Detail information of glow curves, dose responses, and energy responses are essential for the use of TLDs as new dosimeters. Thus, a system has been developed to measure precisely the glow curves and to investigate the characteristics of TLDs in detail. The performance of the system has been investigated by measuring the glow curves and the dose responses of LiF,  $\text{Li}_2\text{B}_4\text{O}_7(\text{Mn})$ , and  $\text{Li}_2\text{B}_4\text{O}_7(\text{Cu})$  TLDs irradiated with  $^{60}\text{Co}$  gamma-rays and synchrotron radiations of 10 to 40 keV up to a couple of  $10^3$  Gy.

In this report, the characteristics of the glow curve measuring system are presented with the measured results of glow curves and dose responses.

## 2. Glow Curve Measuring System of TLDs

The glow curve measuring system is composed of three instruments; a TLD reader unit, a cooling water unit, and an output recording unit, as shown in Fig. 1. A TLD sample in a Pt planchet is heated at a constant rate controlled using the cooling water unit which is equipped with a semiconductor electronic cooling controller. Thermoluminescence (TL) from TLDs is incident to a photomultiplier tube (Hamamatsu R-1288) through two kinds of light filters, resulting photocurrent proportional to the TL intensity. The photocurrent and the TLD temperature monitored by a CA thermocouple on the Pt planchet are digitized with a current digitizer and finally the TL output are sent to an analyzing recorder (Yokogawa 3655E), where a time constant of 1 msec is selected to obtain an optimum S/N ratio of the photocurrent. A infrared filter (HA-30) is generally equipped to remove thermoelectrons emitted from heated components around the TLD, and

## 1. Introduction

Thermoluminescence dosimeters (TLDs) have been used for personal dosimetry of gamma-rays above several tenth keV, and it also has been expected to be a promising one for synchrotron radiations which are very intense X-rays having energies less than several tenth keV, because TLDs have great flexibility in the choice of materials and size. Detail information of glow curves, dose responses, and energy responses are essential for the use of TLDs as new dosimeters. Thus, a system has been developed to measure precisely the glow curves and to investigate the characteristics of TLDs in detail. The performance of the system has been investigated by measuring the glow curves and the dose responses of LiF,  $\text{Li}_2\text{B}_4\text{O}_7(\text{Mn})$ , and  $\text{Li}_2\text{B}_4\text{O}_7(\text{Cu})$  TLDs irradiated with  $^{60}\text{Co}$  gamma-rays and synchrotron radiations of 10 to 40 keV up to a couple of  $10^3$  Gy.

In this report, the characteristics of the glow curve measuring system are presented with the measured results of glow curves and dose responses.

## 2. Glow Curve Measuring System of TLDs

The glow curve measuring system is composed of three instruments; a TLD reader unit, a cooling water unit, and an output recording unit, as shown in Fig. 1. A TLD sample in a Pt planchet is heated at a constant rate controlled using the cooling water unit which is equipped with a semiconductor electronic cooling controller. Thermoluminescence (TL) from TLDs is incident to a photomultiplier tube (Hamamatsu R-1288) through two kinds of light filters, resulting photocurrent proportional to the TL intensity. The photocurrent and the TLD temperature monitored by a CA thermocouple on the Pt planchet are digitized with a current digitizer and finally the TL output are sent to an analyzing recorder (Yokogawa 3655E), where a time constant of 1 msec is selected to obtain an optimum S/N ratio of the photocurrent. A infrared filter (HA-30) is generally equipped to remove thermoelectrons emitted from heated components around the TLD, and

another ultraviolet filter (CS-500 or B-390) pertinent to the wavelength of TL is used to make the background current of the photomultiplier tube decreased. Optical transmission curves of the three filters are shown in Fig. 2. The Pt planchet is a cup of 13 mm diameter and 5 mm depth so that the various types of TLDs of ribbons, pellets, powder and liquid are applicable. Ambient air around the TLD is replaced with  $N_2$  gas to prevent nonradiation induced signals.<sup>1)</sup> This effect was confirmed by measurements as shown in Figs. 3.1 and 3.2. Photo. 1 shows the front panel of the TLD reader unit and the cooling water unit.

The glow curve is represented by the TL intensity vs. the TLD temperature, and the shape is dependent on the temperature rising rate.<sup>2),3),4)</sup> In the present system, the temperature rising rate of TLDs, actually that of the Pt planchet, is controlled by feeding the temperature of the Pt planchet back to the cooling unit from room temperature up to 450 °C, and five different rates; 0.5, 1, 2, 3, and 5 °C/s, are available. The rising rates are rather smaller than those of conventional TLD readers to make the difference of the temperatures between the TLD and the planchet minimized. The profiles of temperature rising at each rate are demonstrated in Figs. 4.1 to 4.5 with the background output of the photomultiplier tube, respectively. The fluctuation of the rising rate becomes maximum for 3 °C/s, but is controlled within an error of almost  $\pm 2$  %.

The dark current of the photomultiplier tube increases with the temperature and depends on the light filter as given in Figs. 3.2, 5.1 and 5.2. The results suggested that the use of a B-390 filter was effective to reduce the dark current due to thermoelectrons with long wavelength which increased greatly at the temperature above 300 °C, although TL signals were absorbed partly by the filter, as well. Two kinds of filters of HA-30 and B-390 usually have been installed.

The selection of a photomultiplier tube is important to realize a TLD reader with low noise and wide measurable range. The Hamamatsu R-1288 photomultiplier tube is sensitive to light with wavelength of 300 to 600 nm covering most TL emission spectra as illustrated in Fig. 6. Optimal high voltage of -1500 volts is recommended to the photomultiplier, but the photomultiplier gain is proportional to the supplied voltage down to -1100 volts as shown in



Fig. 7. Thus, lower high voltage is useful, if the TL output exceeds 100  $\mu\text{A}$ . On the other hand, the background of the present system is less than 0.01 nA as shown in Fig. 3.2 when the two filters of HA-30 and B-390 are used. Consequently, the present system is applicable for wide range covering 7 to 8 orders.

### 3. Application to TLD material research

Glow curves and dose responses for  $^{60}\text{Co}$  gamma-rays and synchrotron radiations have been measured using the present TLD reader system. TLDs used were LiF(TLD-100),  $\text{Li}_2\text{B}_4\text{O}_7\text{:Mn}$ (TLD-800), and  $\text{Li}_2\text{B}_4\text{O}_7\text{(Cu)}$ . The former two were manufactured by Harshaw Chemical Company and the latter by Matsushita Electric Industrial Company. Specification of the TLDs is summarized in Table.1. The chips of LiF and  $\text{Li}_2\text{B}_4\text{O}_7\text{(Cu)}$  were annealed at 400°C for one hour and  $\text{Li}_2\text{B}_4\text{O}_7\text{(Mn)}$  chips annealed at 350°C for 15 minutes in air before irradiation.

#### 3.1 $^{60}\text{Co}$ gamma-ray experiments

Irradiation with  $^{60}\text{Co}$  gamma-rays were carried out using the  $^{60}\text{Co}$  facility in the Japan Atomic Energy Research Institute (JAERI). TLD chips were irradiated between Teflon sheets of 1mm thickness to achieve an electronic equilibrium conditions. The irradiation has been made from  $8.7 \times 10^{-3}$  Gy to 1130 Gy with dose rates from  $1.46 \times 10^{-4}$  Gy/s to 5.33 Gy/s in air where the dose rates were determined with Fricke dosimeters with an accuracy of 10 %. Glow curves of LiF TLDs obtained with heating rates of 1, 2, 3, and 5 °C/s are presented in Figs. 8.1 to 8.4. The results demonstrate that the slower heating rates give the better peak resolution and the peak temperatures shift to the lower side. The temperature shifts are also given in Table 2. Glow curves of LiF,  $\text{Li}_2\text{B}_4\text{O}_7\text{(Mn)}$ , and  $\text{Li}_2\text{B}_4\text{O}_7\text{(Cu)}$  for different dose are represented in Figs. 9.1-9.6, 10.1-10.2 and 11.1-11.3, respectively, where the measurements have been made more than one day later after the irradiation.

It has been reported that a glow curve of LiF is composed of 10<sup>5</sup> or 11 peaks.<sup>6)</sup> All of the peaks, however, have never been

Fig. 7. Thus, lower high voltage is useful, if the TL output exceeds 100  $\mu\text{A}$ . On the other hand, the background of the present system is less than 0.01 nA as shown in Fig. 3.2 when the two filters of HA-30 and B-390 are used. Consequently, the present system is applicable for wide range covering 7 to 8 orders.

### 3. Application to TLD material research

Glow curves and dose responses for  $^{60}\text{Co}$  gamma-rays and synchrotron radiations have been measured using the present TLD reader system. TLDs used were LiF(TLD-100),  $\text{Li}_2\text{B}_4\text{O}_7\text{:Mn}$ (TLD-800), and  $\text{Li}_2\text{B}_4\text{O}_7\text{(Cu)}$ . The former two were manufactured by Harshaw Chemical Company and the latter by Matsushita Electric Industrial Company. Specification of the TLDs is summarized in Table.1. The chips of LiF and  $\text{Li}_2\text{B}_4\text{O}_7\text{(Cu)}$  were annealed at 400°C for one hour and  $\text{Li}_2\text{B}_4\text{O}_7\text{(Mn)}$  chips annealed at 350°C for 15 minutes in air before irradiation.

#### 3.1 $^{60}\text{Co}$ gamma-ray experiments

Irradiation with  $^{60}\text{Co}$  gamma-rays were carried out using the  $^{60}\text{Co}$  facility in the Japan Atomic Energy Research Institute (JAERI). TLD chips were irradiated between Teflon sheets of 1mm thickness to achieve an electronic equilibrium conditions. The irradiation has been made from  $8.7 \times 10^{-3}$  Gy to 1130 Gy with dose rates from  $1.46 \times 10^{-4}$  Gy/s to 5.33 Gy/s in air where the dose rates were determined with Fricke dosimeters with an accuracy of 10 %. Glow curves of LiF TLDs obtained with heating rates of 1, 2, 3, and 5 °C/s are presented in Figs. 8.1 to 8.4. The results demonstrate that the slower heating rates give the better peak resolution and the peak temperatures shift to the lower side. The temperature shifts are also given in Table 2. Glow curves of LiF,  $\text{Li}_2\text{B}_4\text{O}_7\text{(Mn)}$ , and  $\text{Li}_2\text{B}_4\text{O}_7\text{(Cu)}$  for different dose are represented in Figs. 9.1-9.6, 10.1-10.2 and 11.1-11.3, respectively, where the measurements have been made more than one day later after the irradiation.

It has been reported that a glow curve of LiF is composed of 10<sup>5</sup> or 11 peaks.<sup>6)</sup> All of the peaks, however, have never been

observed explicitly by any experiments. In the present measurements, only five peaks have been distinguished clearly as shown in Figs. 8.1 to 8.6, in which the most dominant peak was corresponding to the peak-5 identified by the previous work and the peak-3 and -4 were located at the left side of the peak-5. Lower temperature peak-1 and -2 observed just after the irradiations fade shortly within a day, while higher temperature peak-6 to -10 or -11 classified previously have never been separated apparently despite of the superior resolution of the present glow curve measuring system. The temperatures of the peak-3, -4, and -5 are given in Table 2. The glow curves of Figs. 8.1 to 8.6 also suggest that the high temperature peaks above the main peak become larger with increasing dose.

For  $\text{Li}_2\text{B}_4\text{O}_7(\text{Mn})$  and  $\text{Li}_2\text{B}_4\text{O}_7(\text{Cu})$  TLDs, only one peak was observed and no difference was remarked among the glow curves irradiated with different doses. The peak temperatures observed are summarized in Table 2. The peak temperature of  $\text{Li}_2\text{B}_4\text{O}_7(\text{Cu})$  TLD shifted to higher one with the heating rates as similar to that of  $\text{LiF}$  TLD.

Figures 12, 13 and 14 represent the dose responses of each TLD for  $^{60}\text{Co}$  gamma-rays. The TL intensity denotes the integration of the glow curves. The dose responses are linear up to about 1 Gy for  $\text{LiF}$  TLD and 120 Gy for  $\text{Li}_2\text{B}_4\text{O}_7(\text{Mn})$  TLD, and become supralinear above the doses. While, the response of  $\text{Li}_2\text{B}_4\text{O}_7(\text{Cu})$  TLD shows a linearity up to 650 Gy, and becomes sublinear without any supralinearity. The errors assigned to each data represent the fluctuation of the measured values with plural number of TLDs. The error is within about  $\pm 10\%$  for every TLD which is almost equal to the proper fluctuation in the sensitivity of the TLDs.

### 3.2 Experiments with synchrotron radiations

As similar to the  $^{60}\text{Co}$  gamma-ray experiments, the glow curves and dose responses of the TLDs were measured with respect to monoenergetic 10 keV to 40 keV X-rays taken out from synchrotron radiations of the Photon Factory in the National Laboratory for High Energy Physics (KEK). The experimental configuration is illustrated in Fig. 15. Monoenergetic X-rays are produced with a double crystal

monochromator of Si(1,1,1), and incident to the TLD samples. Two detectors were placed in front of the TLD samples to monitor the absolute intensity of the X-rays and to control higher harmonic X-rays. The absolute intensity monitor is a parallel plate free-air ionization chamber<sup>7)</sup> calibrated with an accuracy of a few % with a total absorption calorimeter.<sup>8)</sup> Monoenergetic X-rays through the monochromator are contaminated inevitably with higher harmonic X-rays carrying an error in the experiments. Thus, the contribution of the higher harmonic X-rays were monitored by measuring a coherent scattered photon spectrum with a HP-Ge detector. A typical scattered photon spectrum for 10 keV X-rays is shown in Fig. 16, in which the higher harmonic X-rays is contributing less than  $4 \times 10^{-4}$ , although it becomes larger with decreasing the X-ray energy of interest. Subsequently, the dose contamination due to the higher energy X-rays was neglected in the present TLD experiments.

The attenuation of X-rays in the 24 cm air path between the center of the free air chamber and the TLDs was taken into account in the evaluation of the exposure of TLDs. Maximum correction was 0.864 for 10 keV X-rays.<sup>9)</sup> Only X-ray beams with a small size are available in the synchrotron radiations, and the intensity has a spatial distribution in the beam. Therefore, the TLD samples were scanned horizontally during the irradiation to irradiate homogeneously.

Dose responses of LiF TLDs have been measured for 10 and 30 keV X-rays as shown in Fig. 12. The supralinearity for 10 keV X-rays is reduced compared with those for 30 keV X-rays and  $^{60}\text{Co}$  gamma-rays. The maximum values of the supralinearity are 3.93 for  $^{60}\text{Co}$  gamma-rays and 2.20 for 10 keV X-rays at about 400 Gy. For 30 keV X-rays, no maximum supralinearity was measured with the irradiation up to 261 Gy .

Glow curves of LiF,  $\text{Li}_2\text{B}_4\text{O}_7(\text{Mn})$ , and  $\text{Li}_2\text{B}_4\text{O}_7(\text{Cu})$  TLDs for 10 to 40 keV X-rays are represented in Figs. 17.1-17.10, 18.1-18.7, and 19.1-19.7. As for LiF TLDs, the contribution of higher temperature peaks for low energy X-rays is relatively larger than that for  $^{60}\text{Co}$  gamma-rays, and increases with the dose as similar to that for  $^{60}\text{Co}$  gamma-rays. Only one peak was observed for  $\text{Li}_2\text{B}_4\text{O}_7(\text{Mn})$  TLD.

#### 4. Conclusion

A glow curve measuring system of TLD has been developed, and the excellent properties were demonstrated with the measurements of glow curves and dose responses of LiF,  $\text{Li}_2\text{B}_4\text{O}_7(\text{Mn})$ , and  $\text{Li}_2\text{B}_4\text{O}_7(\text{Cu})$  TLDs for  $^{60}\text{Co}$  gamma-rays and synchrotron radiations from 10 to 40 keV. The glow curves for various TLDs can be obtained with different constant heating rates. In addition, the glow curve is recorded as digital data to be analyzed easily and accurately with aid of a computer which is very useful for the basic research of TLDs including TL mechanism. Besides, it was demonstrated with the dose response measurements of LiF,  $\text{Li}_2\text{B}_4\text{O}_7(\text{Mn})$ , and  $\text{Li}_2\text{B}_4\text{O}_7(\text{Cu})$  TLDs that the present system was useful for wide range over 7 decades. Hence we have acquired a definite outlook that the present glow curve measuring system will make the TLDs realized for synchrotron radiation dosimetry.

#### Acknowledgments

We would like to express great thanks to K. Watai of Oyo Koken Industrial Company for his design and production of the TLD reader units. We wish to thank T. Okubo of the Solid Chemistry Section in JAERI for TLD irradiation with  $^{60}\text{Co}$  gamma-rays. H. Kawada and N. Watanabe of KEK should be appreciated for their great assistance in the experiments at the Photon Factory.

#### 4. Conclusion

A glow curve measuring system of TLD has been developed, and the excellent properties were demonstrated with the measurements of glow curves and dose responses of LiF,  $\text{Li}_2\text{B}_4\text{O}_7(\text{Mn})$ , and  $\text{Li}_2\text{B}_4\text{O}_7(\text{Cu})$  TLDs for  $^{60}\text{Co}$  gamma-rays and synchrotron radiations from 10 to 40 keV. The glow curves for various TLDs can be obtained with different constant heating rates. In addition, the glow curve is recorded as digital data to be analyzed easily and accurately with aid of a computer which is very useful for the basic research of TLDs including TL mechanism. Besides, it was demonstrated with the dose response measurements of LiF,  $\text{Li}_2\text{B}_4\text{O}_7(\text{Mn})$ , and  $\text{Li}_2\text{B}_4\text{O}_7(\text{Cu})$  TLDs that the present system was useful for wide range over 7 decades. Hence we have acquired a definite outlook that the present glow curve measuring system will make the TLDs realized for synchrotron radiation dosimetry.

#### Acknowledgments

We would like to express great thanks to K. Watai of Oyo Koken Industrial Company for his design and production of the TLD reader units. We wish to thank T. Okubo of the Solid Chemistry Section in JAERI for TLD irradiation with  $^{60}\text{Co}$  gamma-rays. H. Kawada and N. Watanabe of KEK should be appreciated for their great assistance in the experiments at the Photon Factory.

## References

- 1) Svarcer V. and Fowler J.F.: "Spurious thermoluminescence and tribothermoluminescence in lithium fluoride dosimetry powder", Proc. Int. Conf. Luminescence Dosimetry, CONF-650637, 227 (1967)
- 2) Gorbics S.G., Nash A.E., and Attix F.H.: "Thermal quenching of luminescence in six thermoluminescent dosimetry phosphors-II", Int. J. Appl. Radiat. Isot., 20, 843 (1969)
- 3) Taylor G.C. and Lilley E.: "The analysis of thermoluminescent glow peaks in LiF(TLD-100)", J. Phys. D: Appl. Phys., 11, 567 (1978)
- 4) Taylor G.C. and Lilley E.: "Rapid readout rate studies of thermoluminescence in LiF(TLD-100) crystals:III", J. Phys. D: Appl. Phys., 15, 2053 (1982)
- 5) Jain V.K., Kathuria S.P., and Ganguly A.K.: "Radiation damage in thermoluminescent LiF-TLD phosphor", J. Phys. C: Solid State Phys., 8, 2191 (1975)
- 6) Fairchild R.G., et al. : " Thermoluminescence of LiF TLD-100:Glow-curve kinetics", J. Appl. Phys., 49(8), 4523 (1978)
- 7) Ban S., et al. : " Measurement of Photon Energy Absorption Coefficient of Air, Nitrogen and Argon at 30 keV", to be submitted to Int. J. Appl. Radiat. Isot.
- 8) Nakashima H., et al.: " Development of a microcalorimeter for measuring absolute intensity of synchrotron radiation", Nucl. Inst. Meth., A310, 696 (1991)
- 9) Hubbell J.H.:" Photon Mass Attenuation and Energy-absorption Coefficients from 1 keV to 20 MeV", Int. J. Appl. Radiat. Isot. 33, 1269 (1982)

Table 1 Specification of TLDs

Material	Dimensions (mm)	Emission spectra (nm)	Filter used
LiF	3.2x3.2x0.38	350-600(max. 400)	HA-30 + B-390
Li <sub>2</sub> B <sub>4</sub> O <sub>7</sub> (Mn)	3.2x3.2x0.89	530-630(max. 605)	HA-30 + CS-500
Li <sub>2</sub> B <sub>4</sub> O <sub>7</sub> (Cu)	3φx0.065 (on a 80 μm-thick polyimide film)	310-440(max. 368)	HA-30 + B-390

Table 2 Peak temperatures of TLDs  
irradiated with <sup>60</sup>Co gamma-rays

Materials	Heating rates (°C/s)			
	1	2	3	5
LiF				
peak-3	178	188	197	216
peak-4	213	226	234	250
peak-5	238	248	256	269
Li <sub>2</sub> B <sub>4</sub> O <sub>7</sub> (Mn)		200		
Li <sub>2</sub> B <sub>4</sub> O <sub>7</sub> (Cu)	250	265		290

(unit: °C)



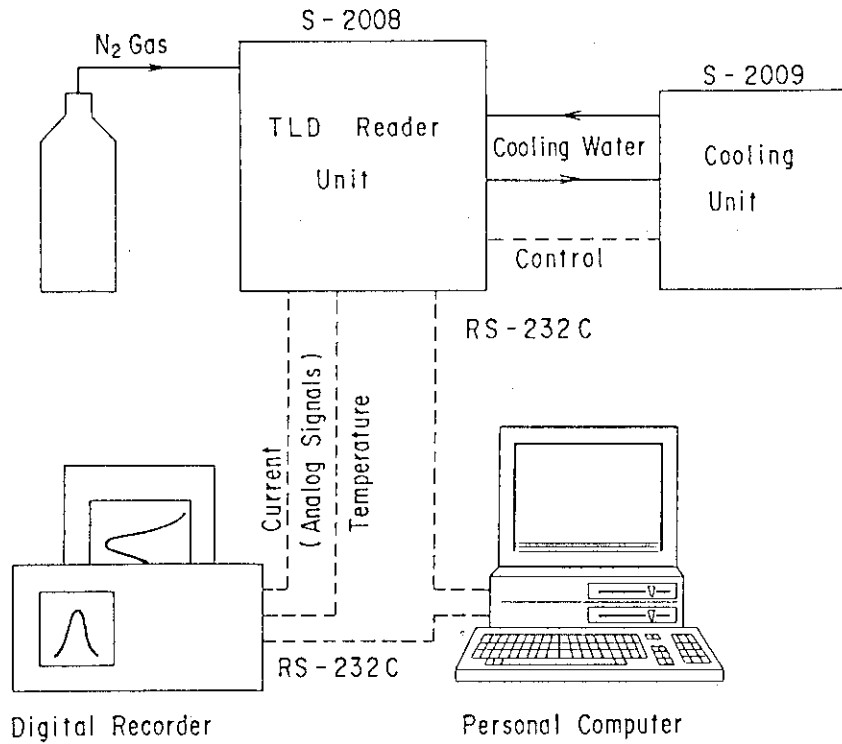


Fig. 1 Block diagram of the TLD glow curve measuring system.

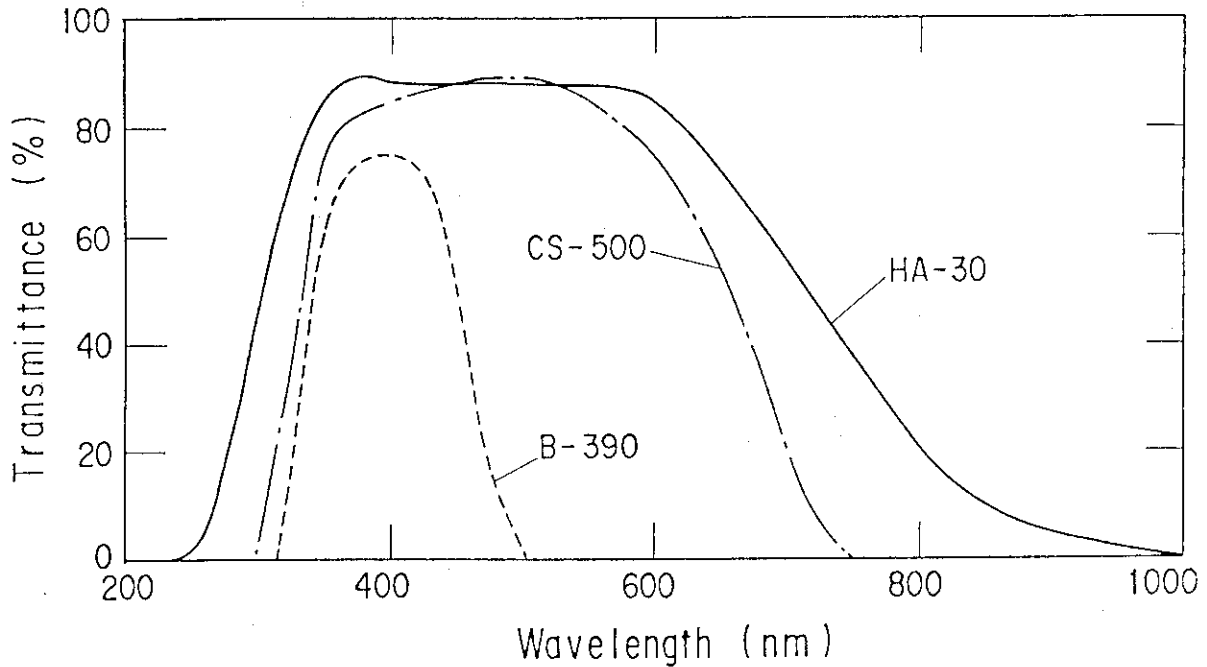


Fig. 2 Optical transmission curves for each filters ; HOYA color filter glass HA-30, CS-500, and B-390.

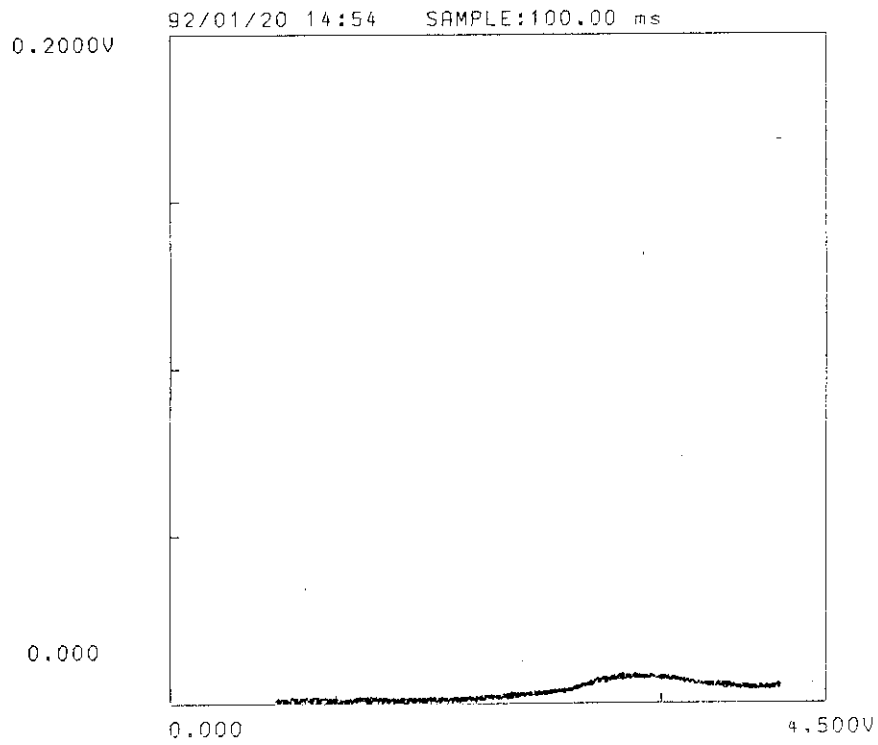


Fig. 3.1 Noise without  $N_2$  gas flow using HA-30 and B-390 filters at a heating of  $2^\circ\text{C/s}$ .

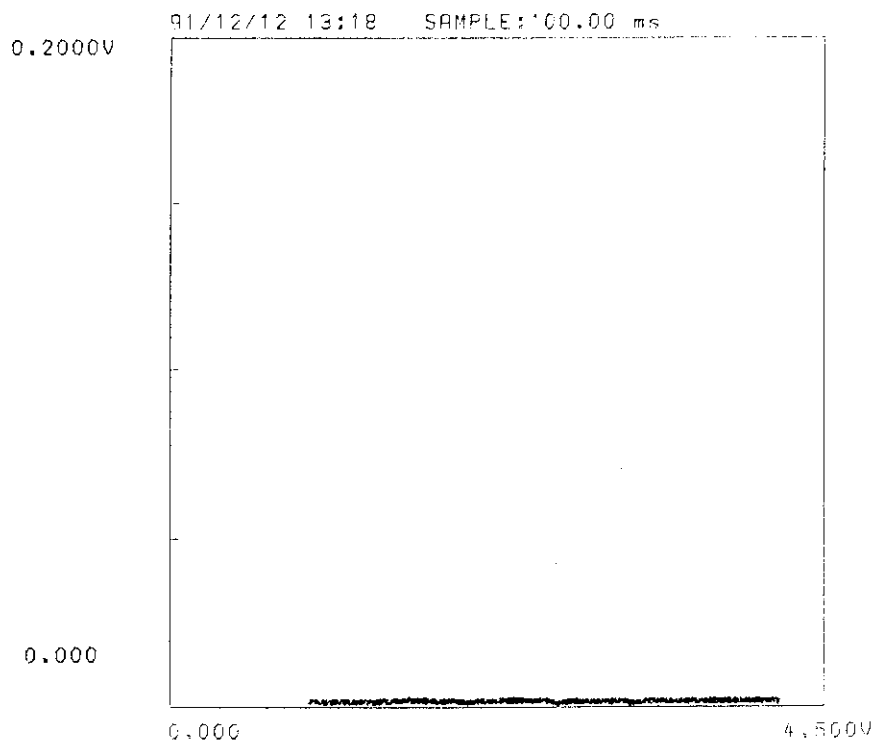


Fig. 3.2 Noise with  $N_2$  gas flow using HA-30 and B-390 filters at a heating rate of  $2^\circ\text{C/s}$ .

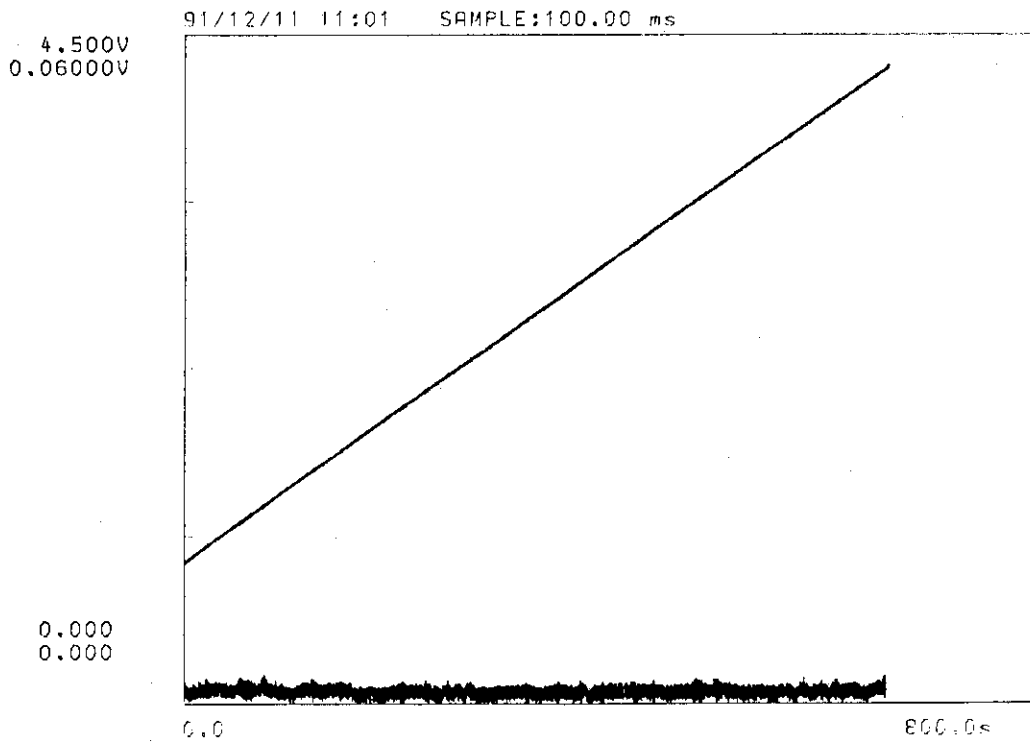


Fig. 4.1 A time-temperature profile for a heating rate of  $0.5^{\circ}\text{C/s}$ . The lower curve shows the background output of the photocurrent tube.

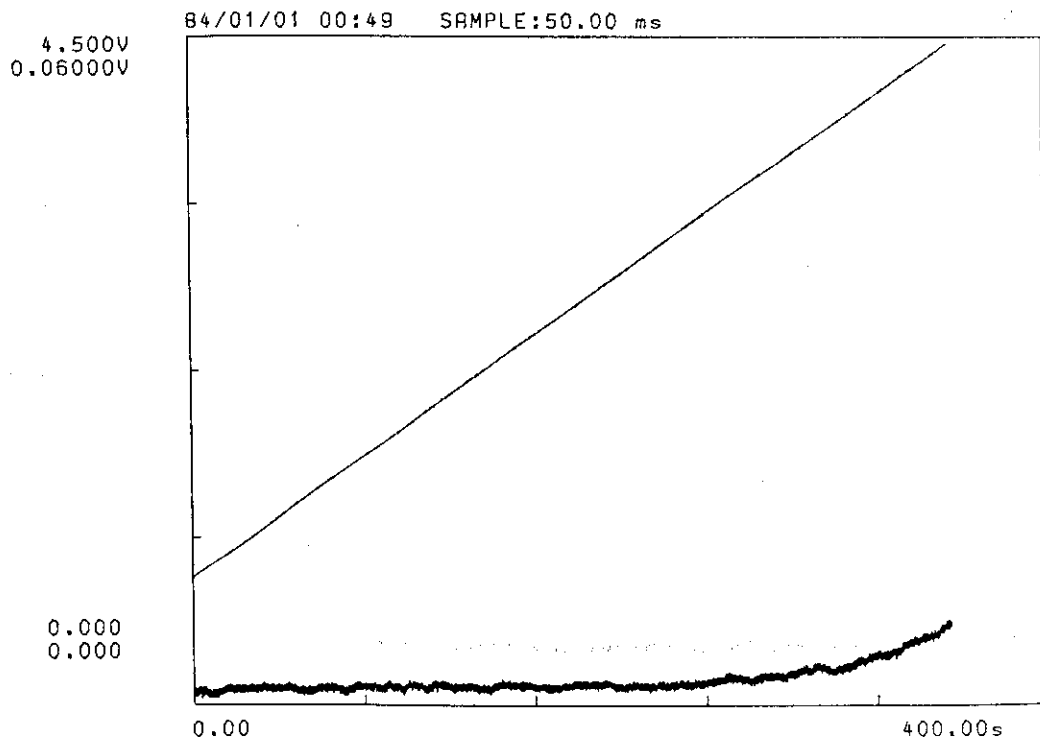


Fig. 4.2 A time-temperature profile for a heating rate of  $1^{\circ}\text{C/s}$ .

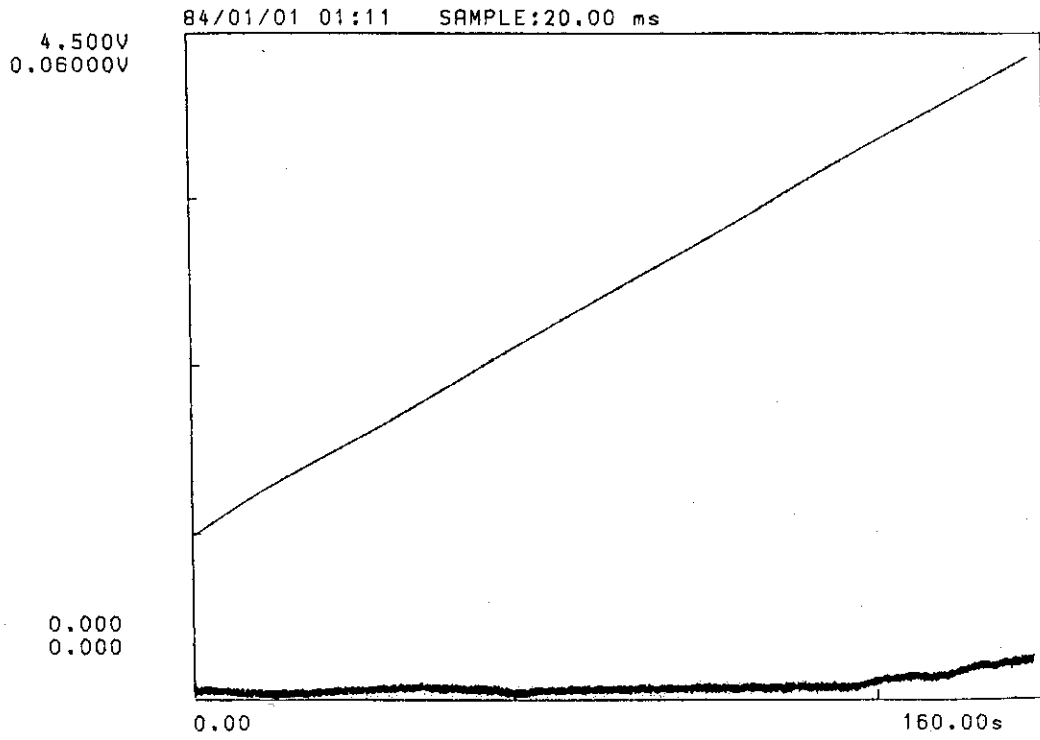


Fig. 4.3 A time-temperature profile for a heating rate of 2°C/s.

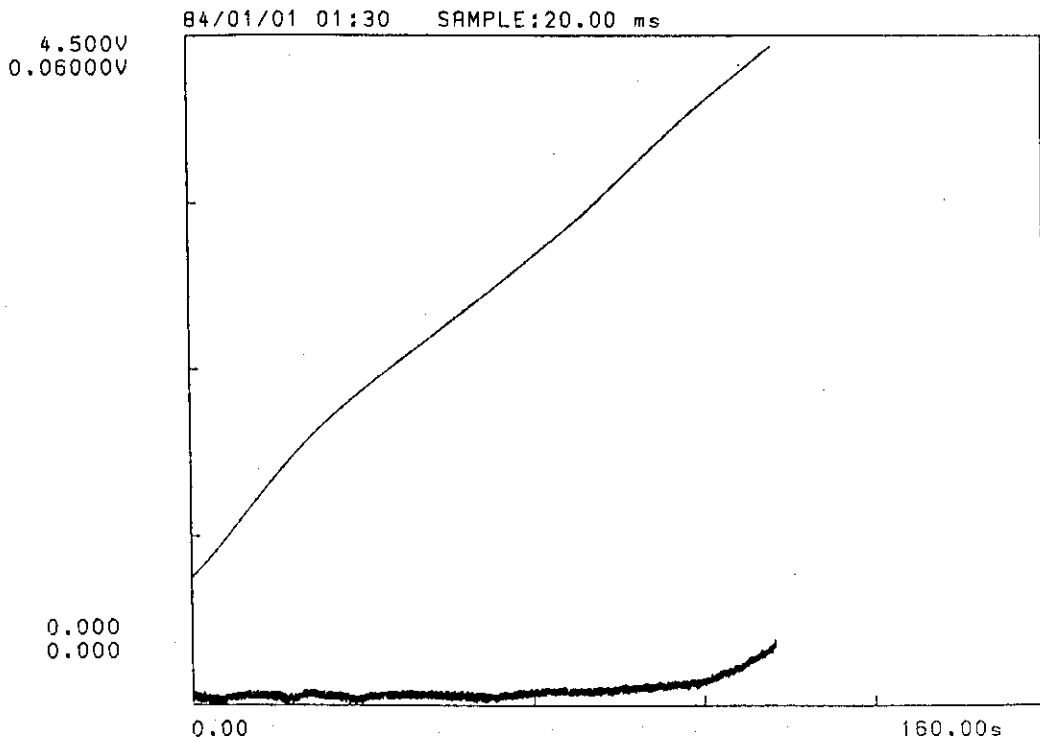


Fig. 4.4 A time-temperature profile for a heating rate of 3°C/s.

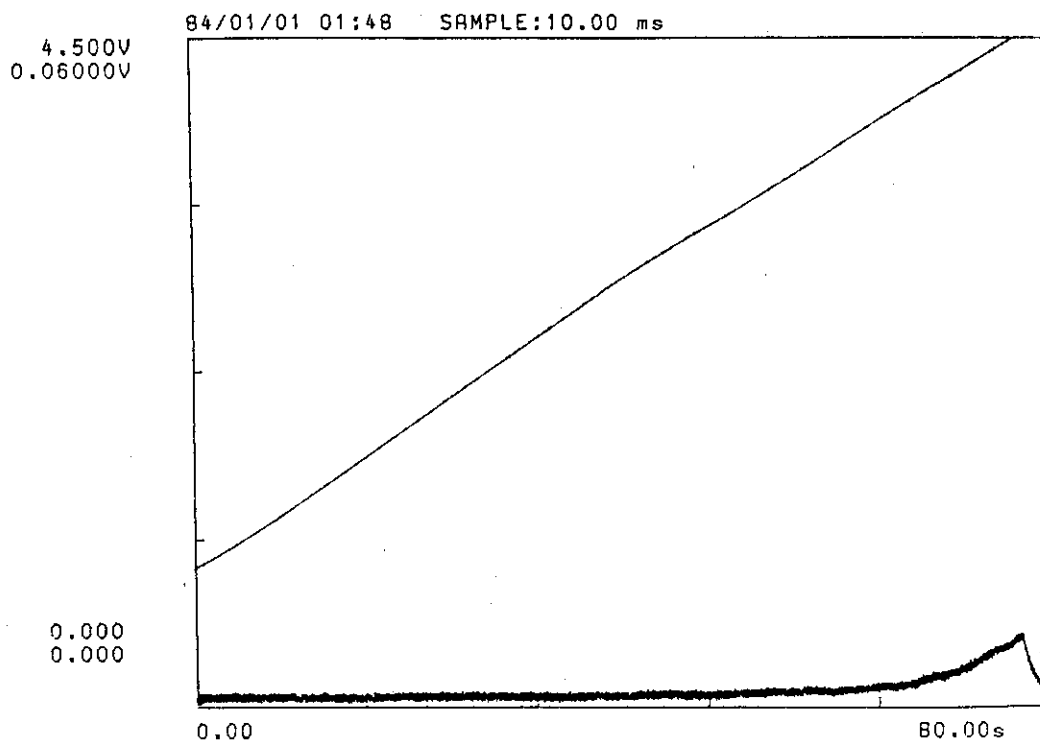


Fig. 4.5 A time-temperature profile for a heating rate of 5°C/s.

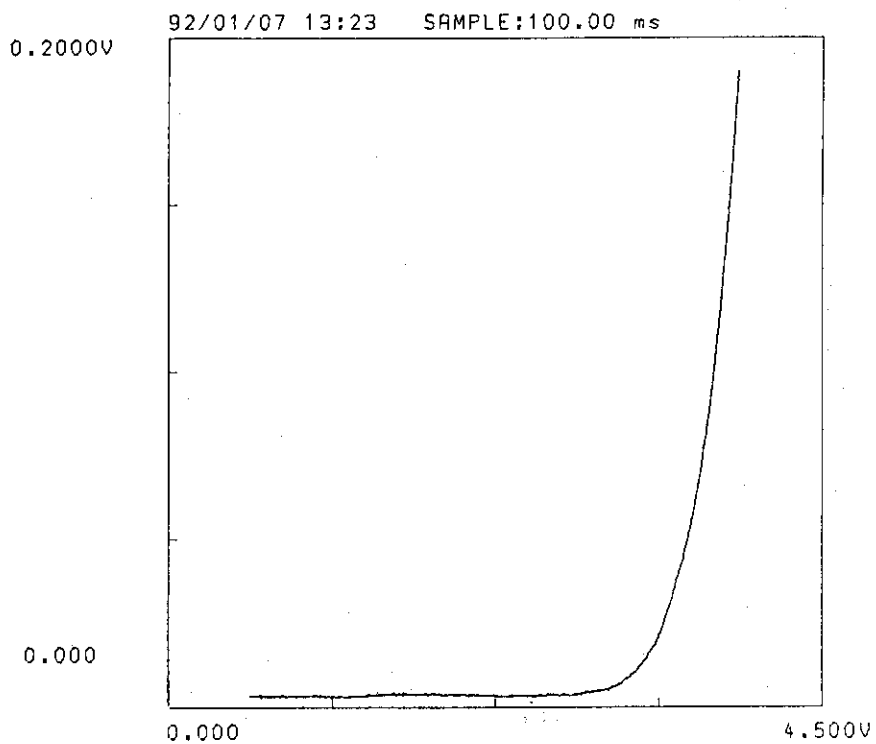


Fig. 5.1 Noise with a infrared filter (HA-30) at a heating rate of 2°C/s.

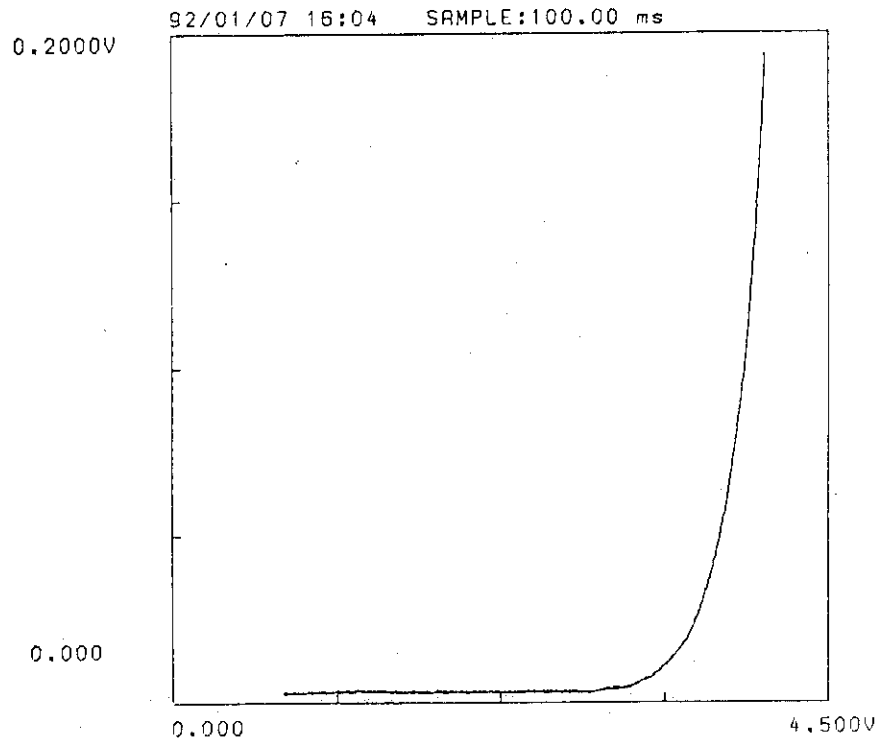


Fig. 5.2 Noise with the two filters of HA-30 and CS-500 at a heating rate of 2°C/s.

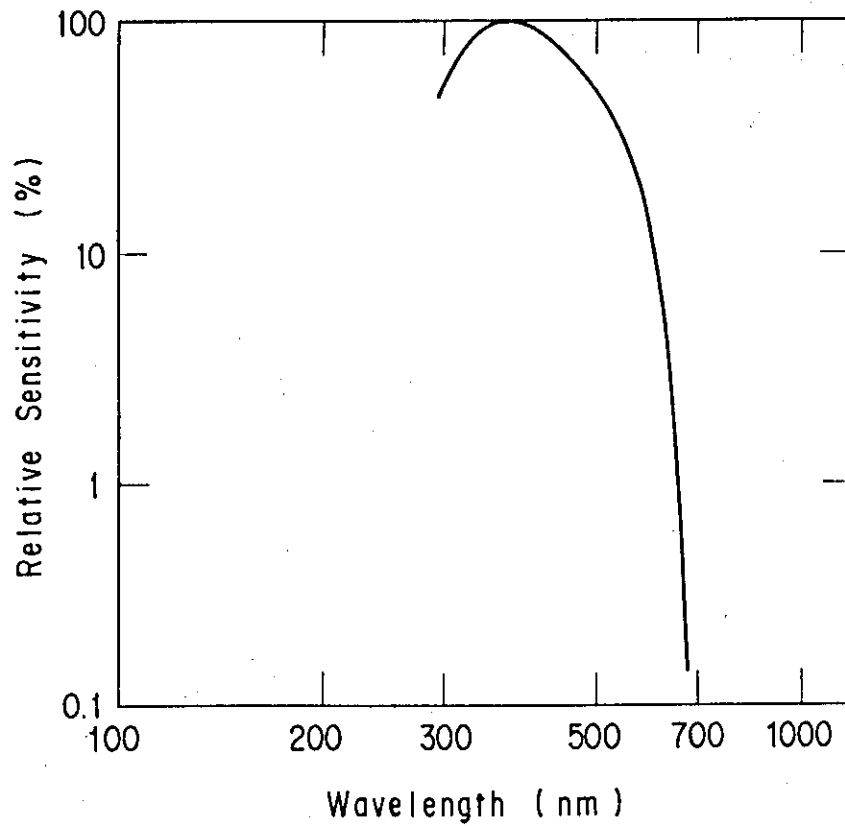


Fig. 6 Relative sensitivity of the photomultiplier tube (Hamamatsu R-1288) as a function of light wavelength.

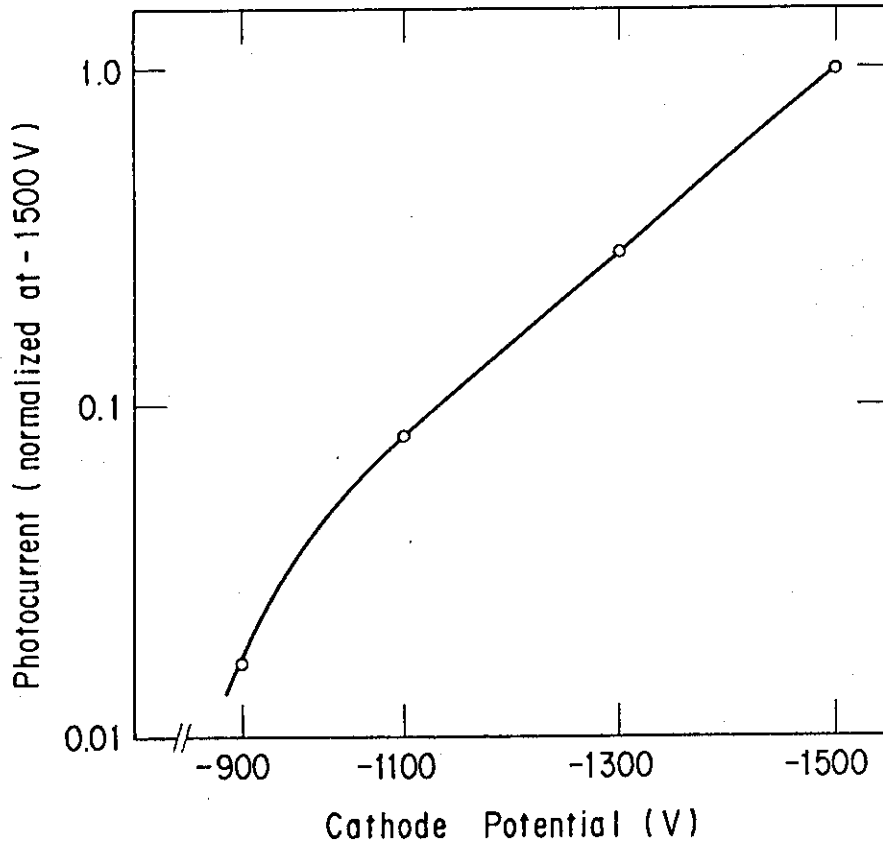


Fig. 7 Photocurrent dependence of supplied voltages. It shows that voltage between -1100 V and -1500 V can be used for measurements.

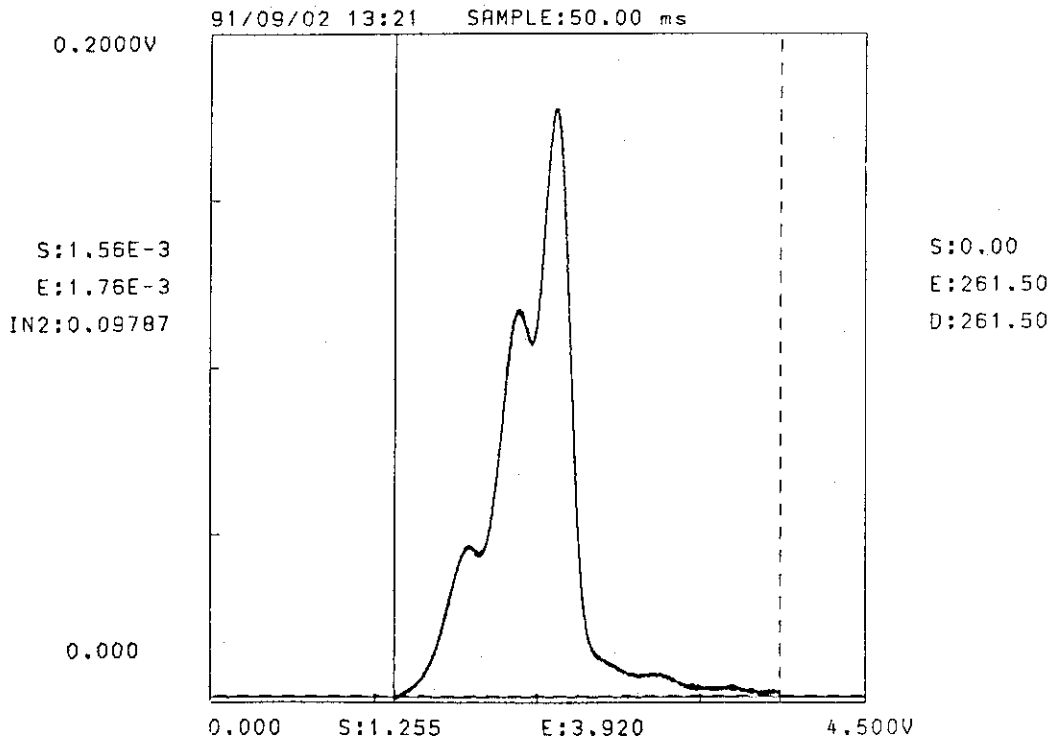


Fig. 8.1 A typical glow curve of LiF to  $^{60}\text{Co}$  gamma-rays at a heating rate of  $1^\circ\text{C/s}$ . The x-axis shows temperatures with a conversion factor of  $100^\circ\text{C/V}$ . "SAMPLE" means a sampling rate of the digital recorder and "IN2" a integration value of the glow curve.

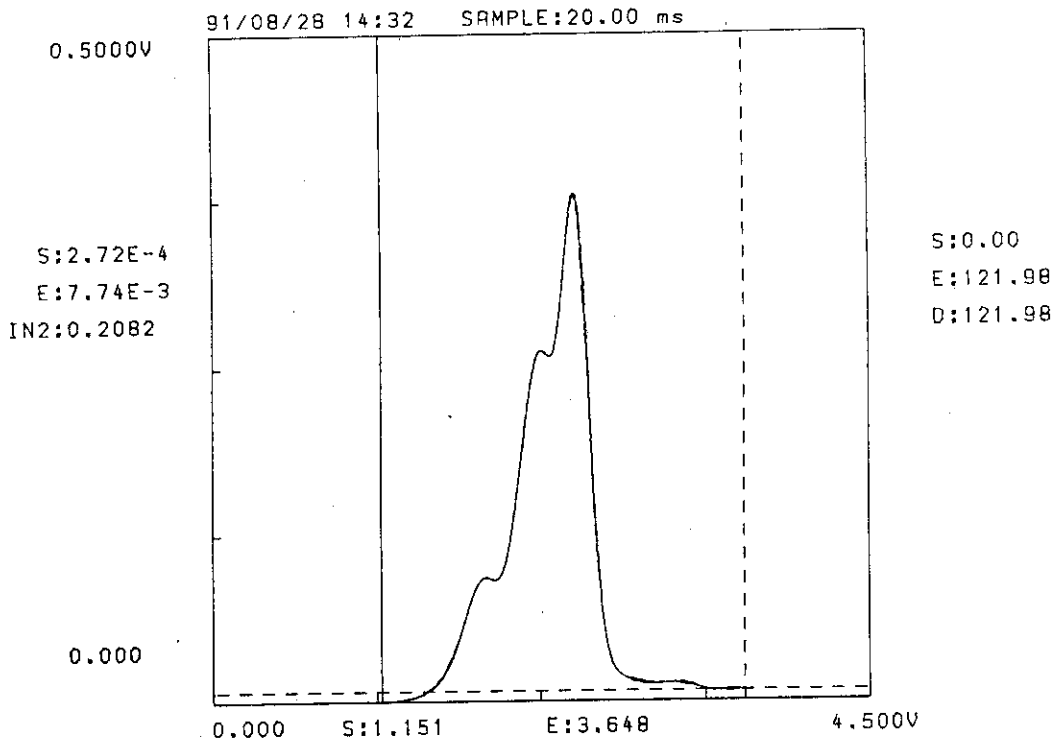


Fig. 8.2 A typical glow curve of LiF to  $^{60}\text{Co}$  gamma-rays at a heating rate of  $2^\circ\text{C/s}$ .

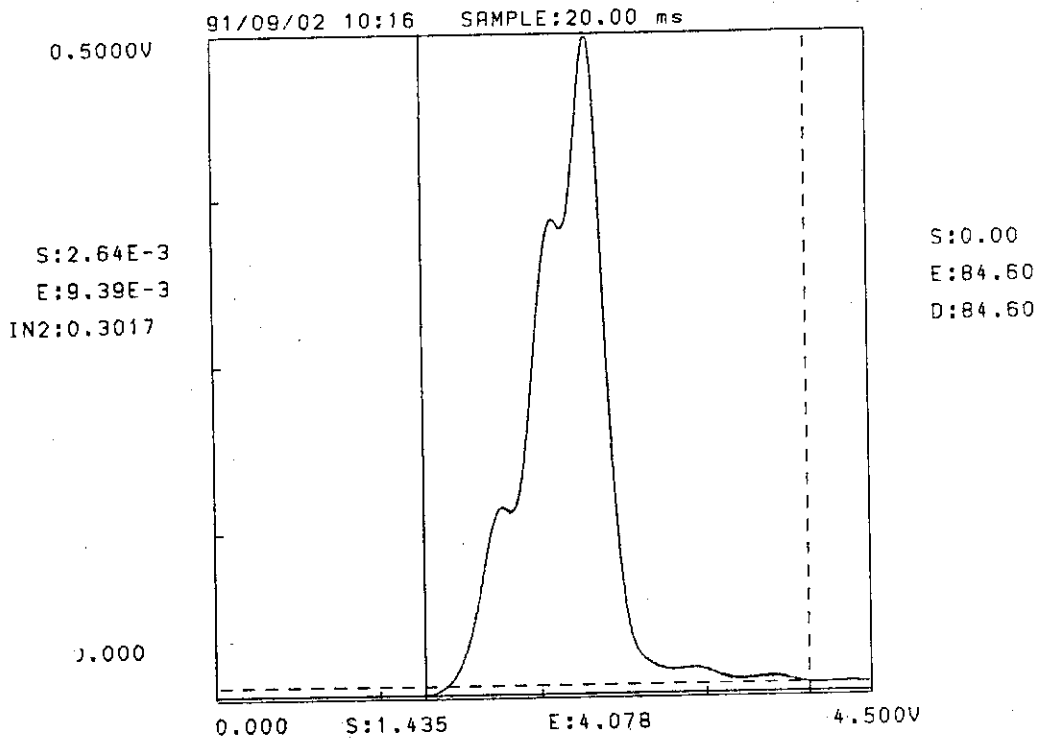


Fig. 8.3 A typical glow curve of LiF to  $^{60}\text{Co}$  gamma-rays at a heating rate of  $3^\circ\text{C/s}$ .



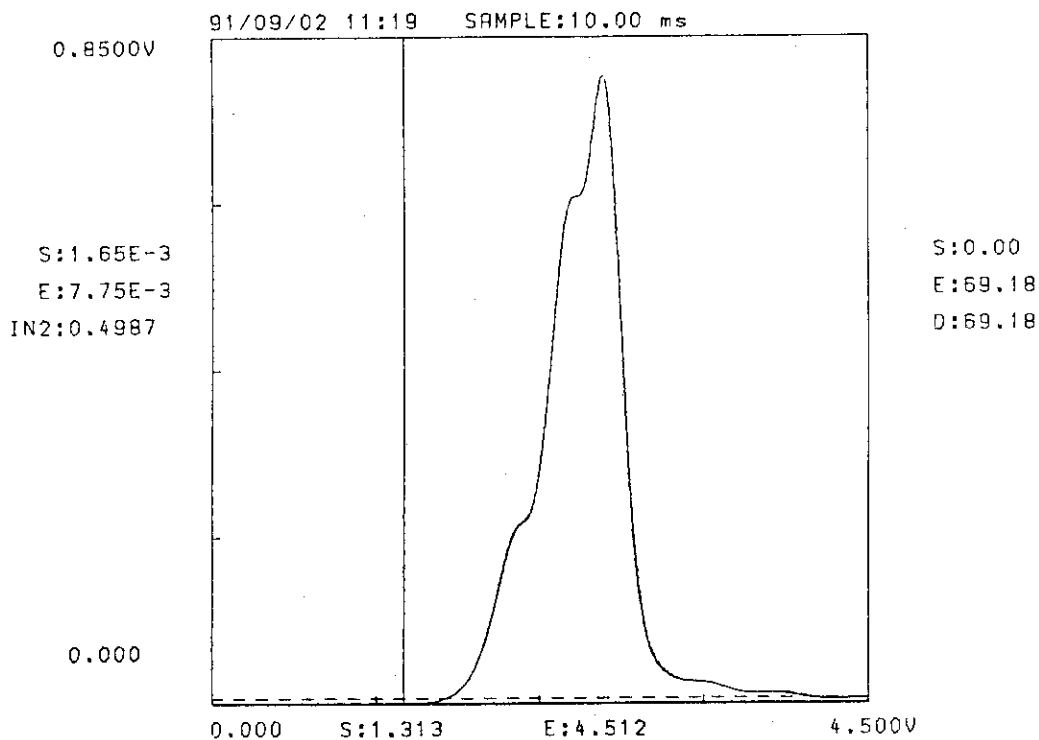


Fig. 8.4 A typical glow curve of LiF to  $^{60}\text{Co}$  gamma-rays at a heating rate of  $5^\circ\text{C/s}$ . Peak-3 and -4 are not shown clearly.

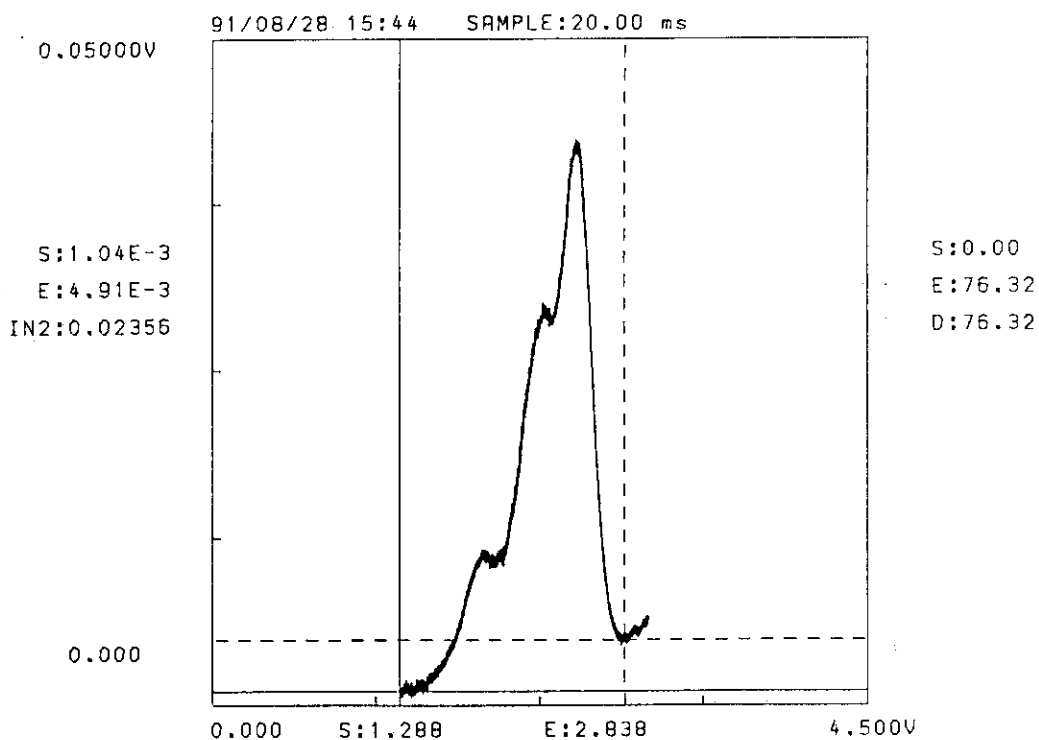


Fig. 9.1 A typical glow curve of LiF at  $8.73 \times 10^{-3}$  Gy of  $^{60}\text{Co}$  gamma-rays. A heating rate of  $2^\circ\text{C/s}$  was used.

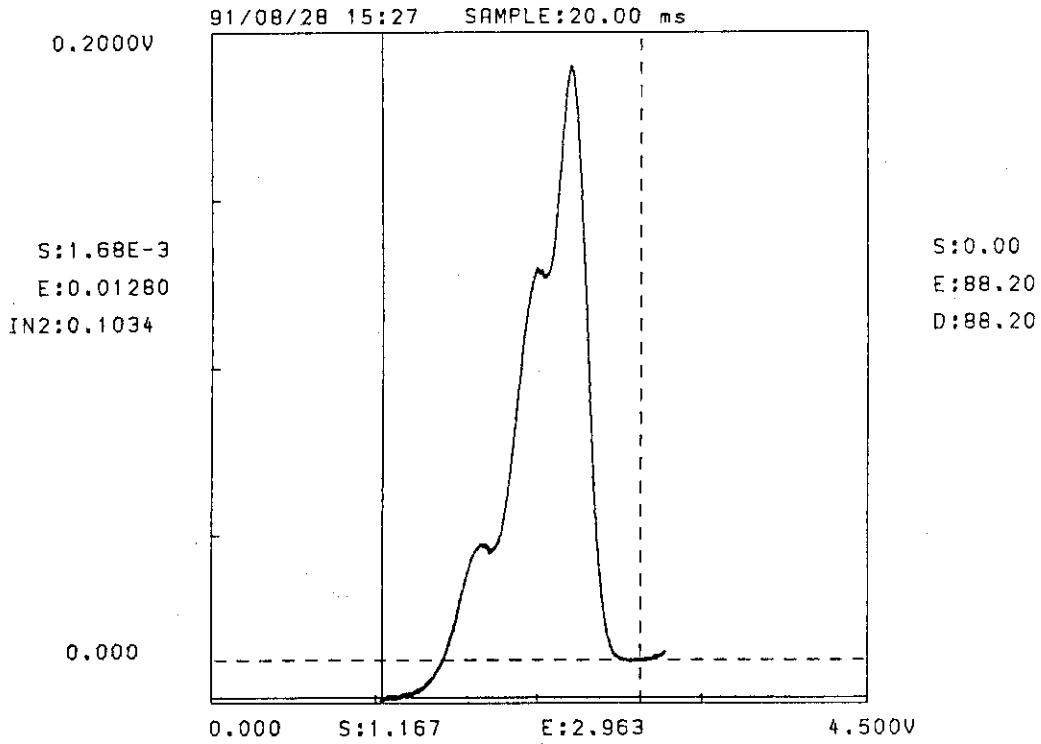


Fig. 9.2 A typical glow curve of LiF at  $4.37 \times 10^{-2}$  Gy of  $^{60}\text{Co}$  gamma-rays.

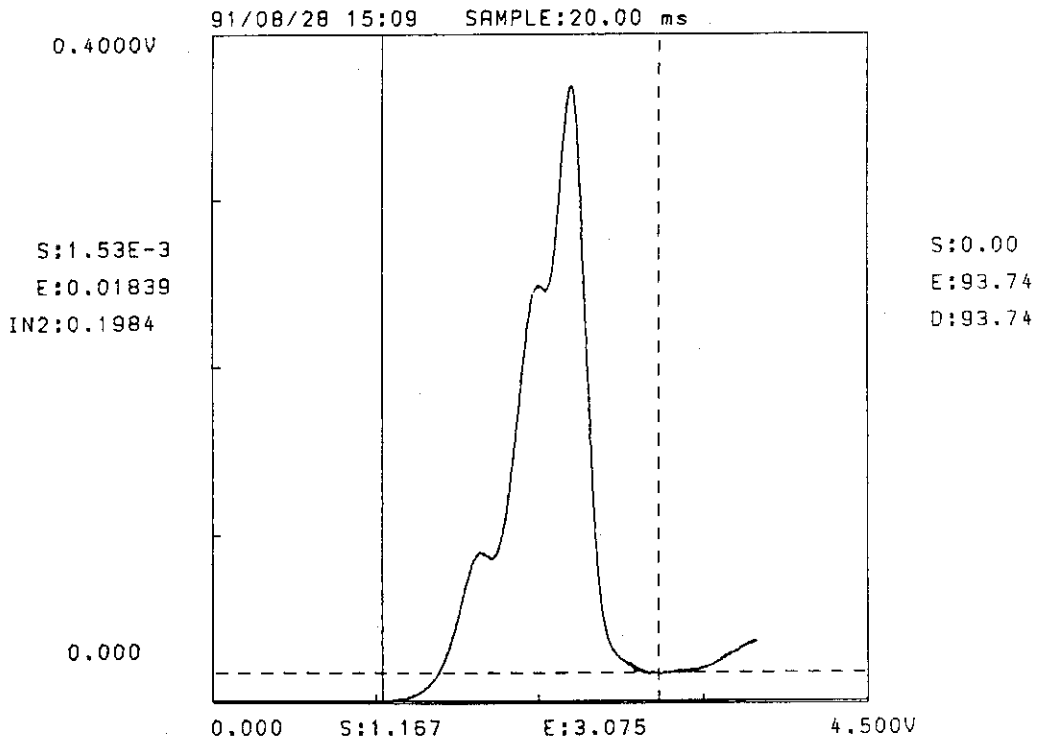


Fig. 9.3 A typical glow curve of LiF at  $8.73 \times 10^{-2}$  Gy of  $^{60}\text{Co}$  gamma-rays.

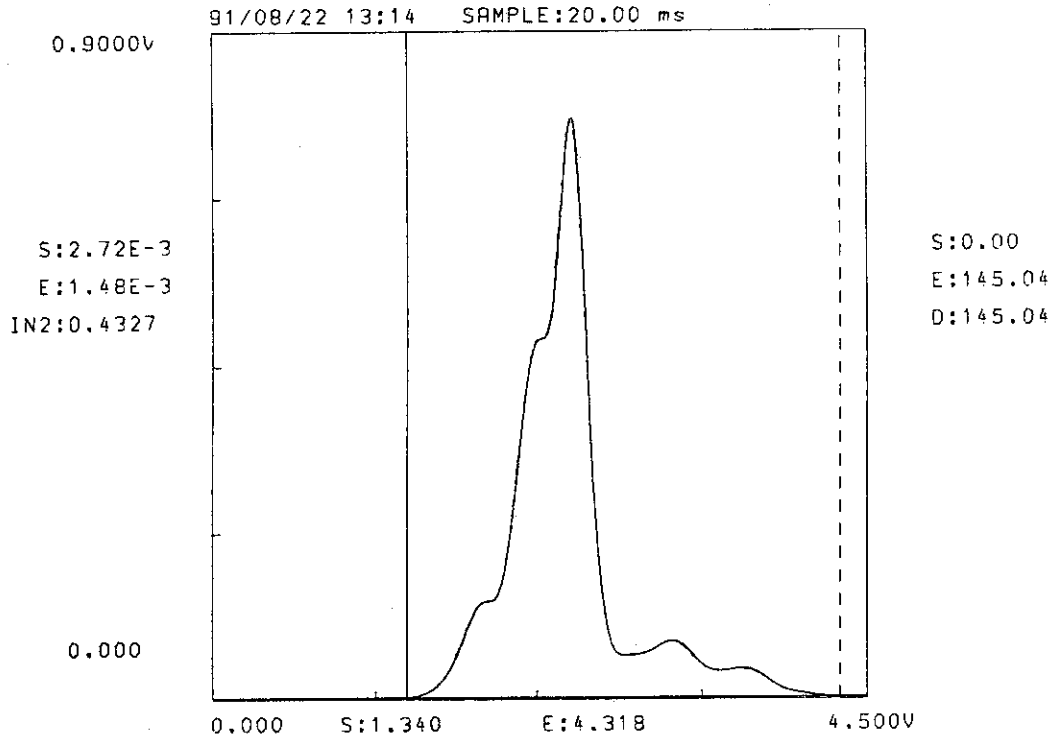


Fig. 9.4 A typical glow curve of LiF at  $8.47 \times 10^1$  Gy of  $^{60}\text{Co}$  gamma-rays.

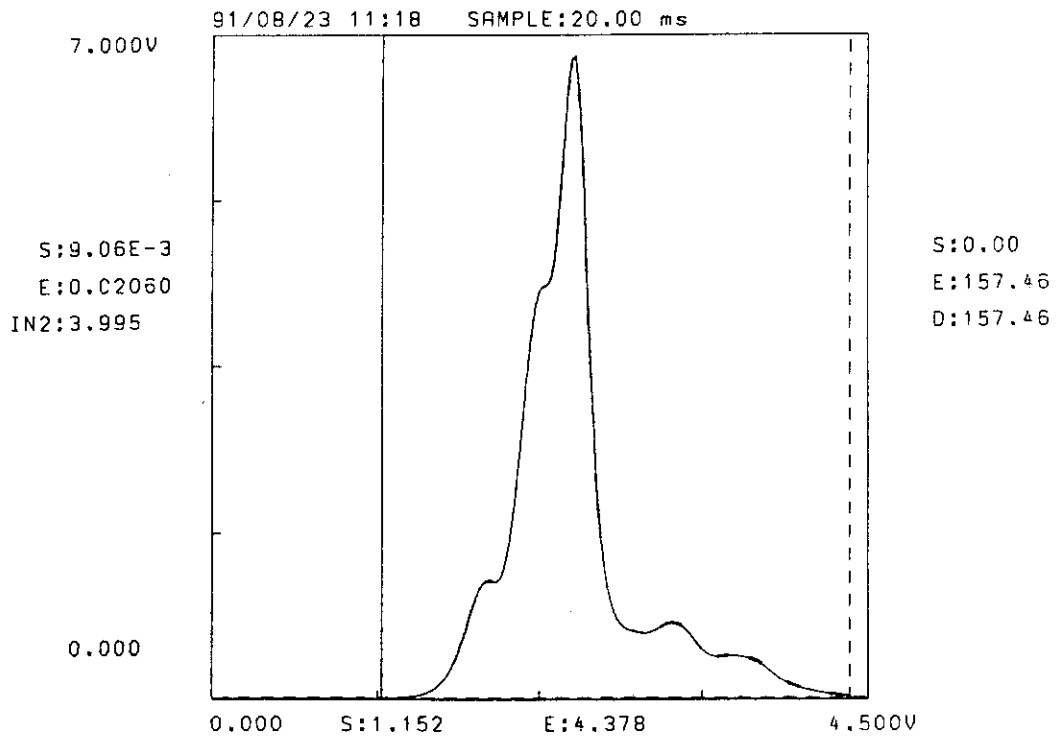


Fig. 9.5 A typical glow curve of LiF at  $4.19 \times 10^2$  Gy of  $^{60}\text{Co}$  gamma-rays.

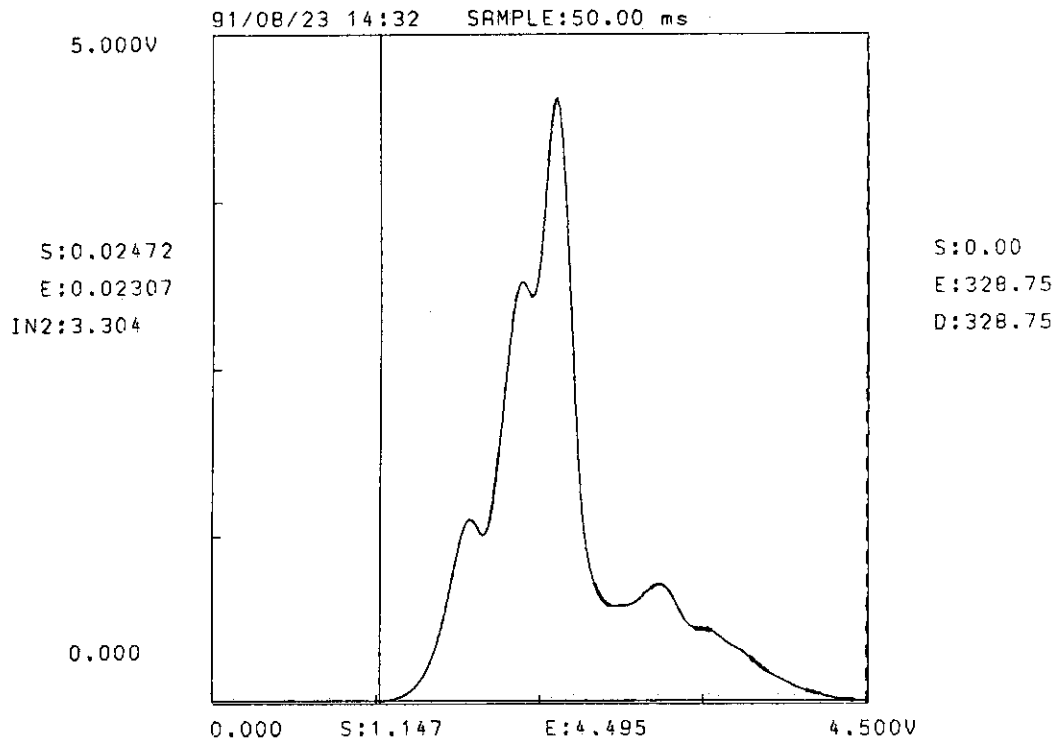


Fig. 9.6 A typical glow curve of LiF at  $1.13 \times 10^3$  Gy of  $^{60}\text{Co}$  gamma-rays. A heating rate of  $2^\circ\text{C/s}$  was used.

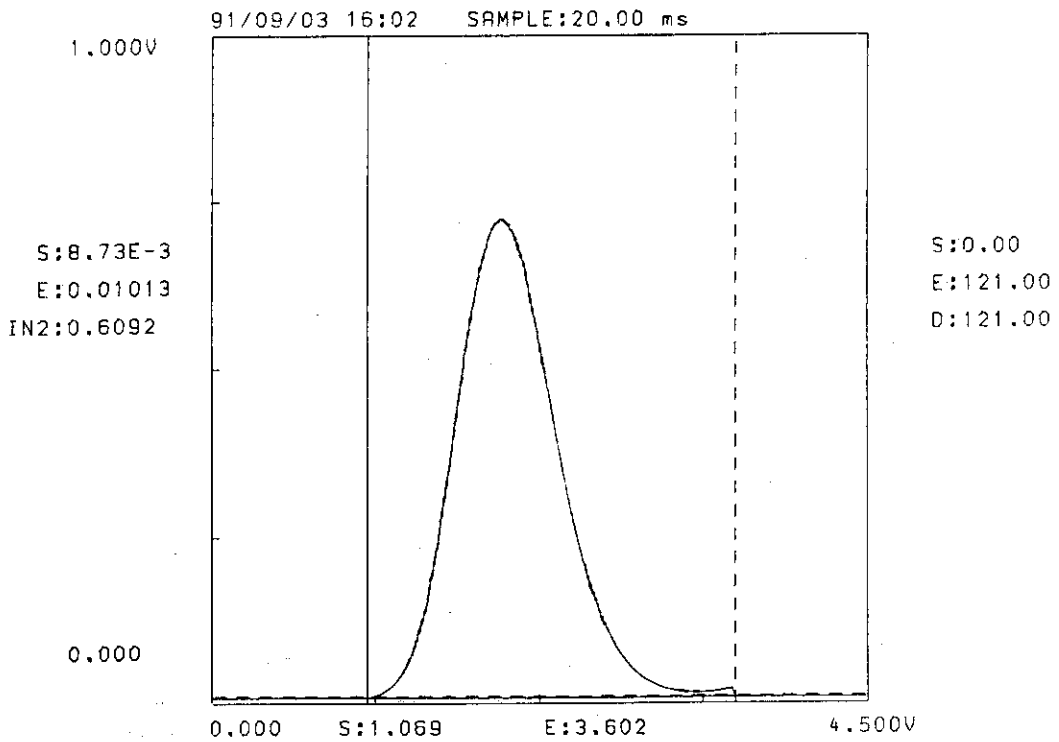


Fig. 10.1 A typical glow curve of  $\text{Li}_2\text{B}_4\text{O}_7(\text{Mn})$  at 5.24 Gy of  $^{60}\text{Co}$  gamma-rays. A heating rate of  $2^\circ\text{C/s}$  was used.

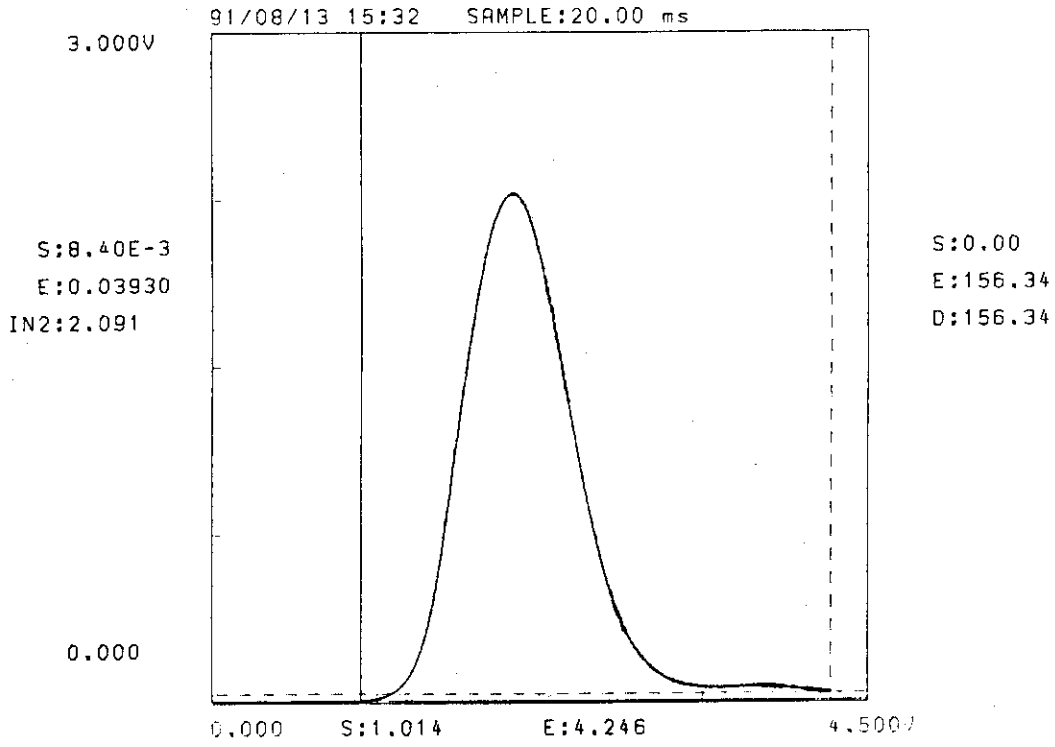


Fig. 10.2 A typical glow curve of  $\text{Li}_2\text{B}_4\text{O}_7(\text{Mn})$  at  $1.13 \times 10^3$  Gy of  $^{60}\text{Co}$  gamma-rays.

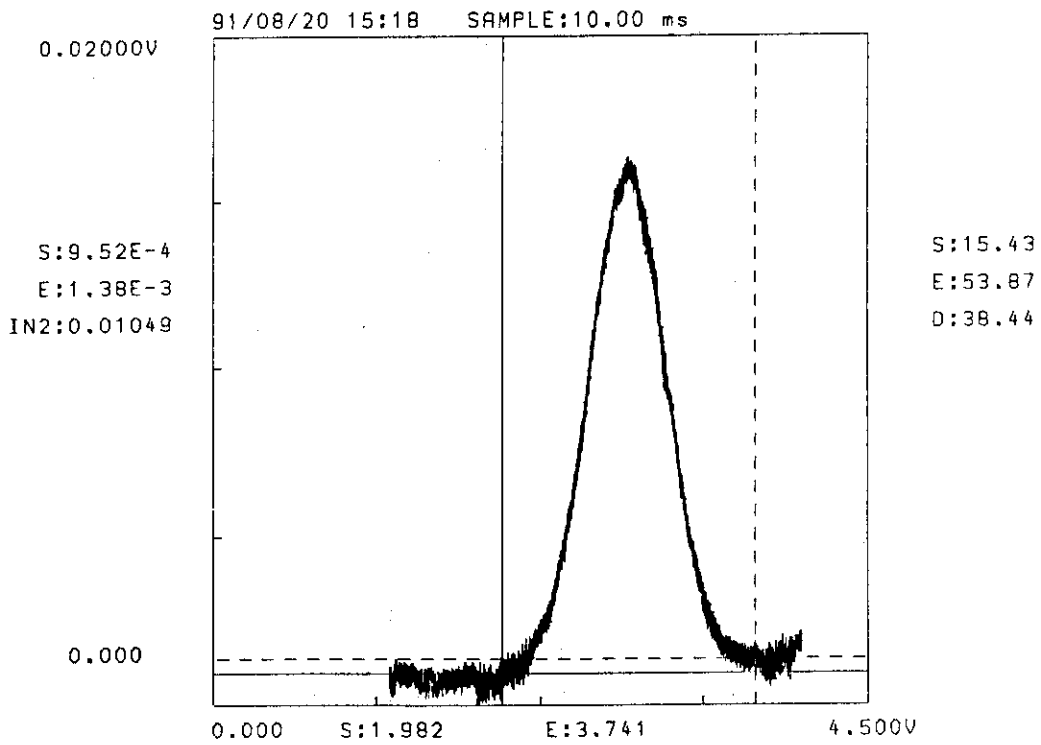


Fig. 11.1 A typical glow curve of  $\text{Li}_2\text{B}_4\text{O}_7(\text{Cu})$  at  $4.37 \times 10^{-2}$  Gy of  $^{60}\text{Co}$  gamma-rays. A heating rate of  $5^\circ\text{C/s}$  was used.

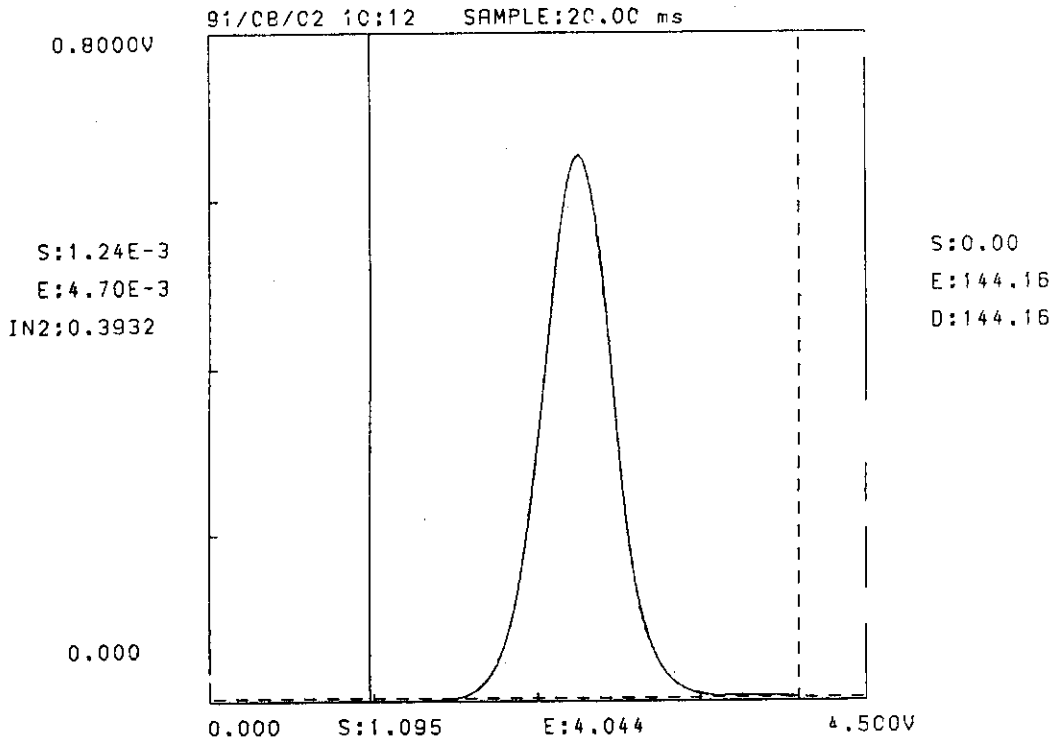


Fig. 11.2 A typical glow curve of  $\text{Li}_2\text{B}_4\text{O}_7(\text{Cu})$  at  $3.14 \times 10^2$  Gy of  $^{60}\text{Co}$  gamma-rays. A heating rate of  $2^\circ\text{C/s}$  was used.

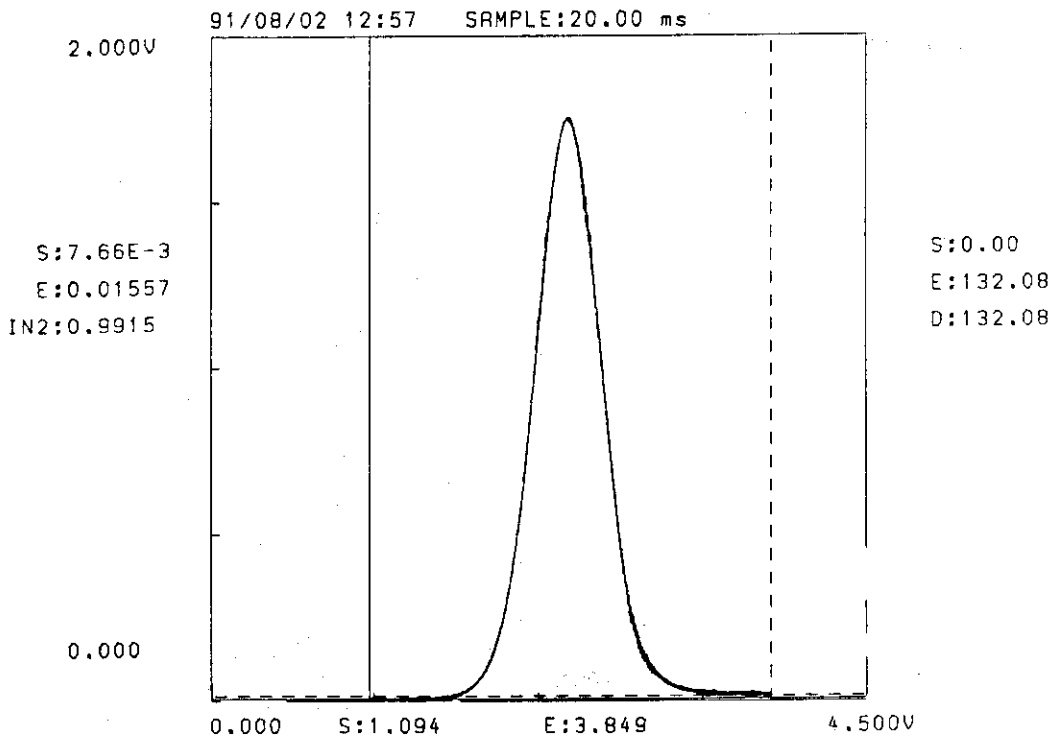


Fig. 11.3 A typical glow curve of  $\text{Li}_2\text{B}_4\text{O}_7(\text{Cu})$  at  $1.13 \times 10^3$  Gy of  $^{60}\text{Co}$  gamma-rays.

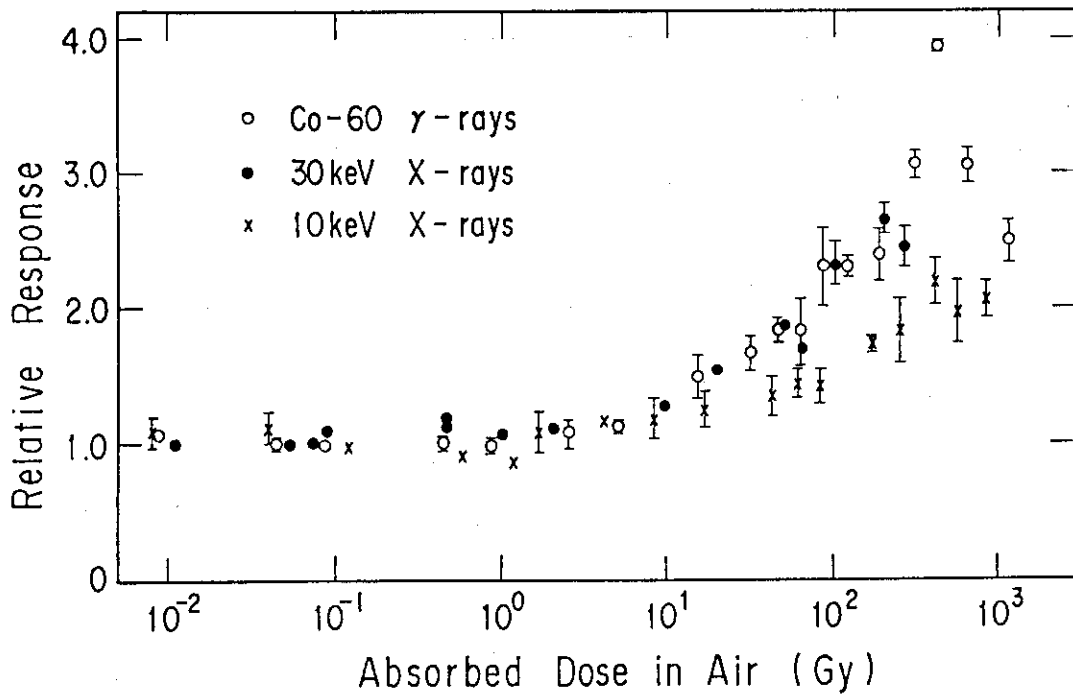


Fig. 12 TL dose responses of LiF to  $^{60}\text{Co}$  gamma-rays, 30 keV, and 10 keV X-rays.

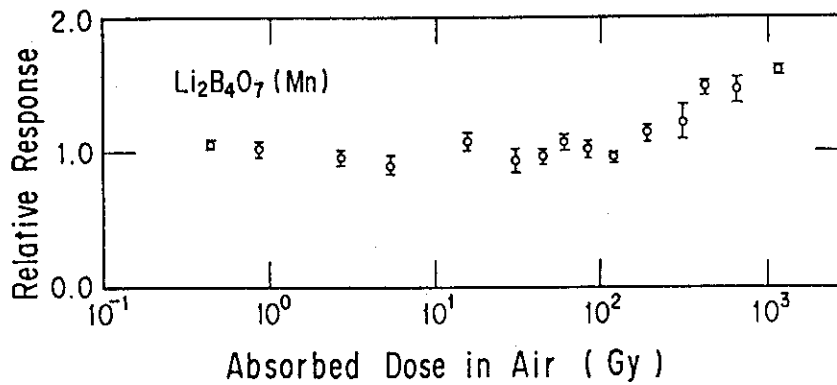


Fig. 13 TL dose response of  $\text{Li}_2\text{B}_4\text{O}_7(\text{Mn})$  to  $^{60}\text{Co}$  gamma-rays. Supralinearity was observed.

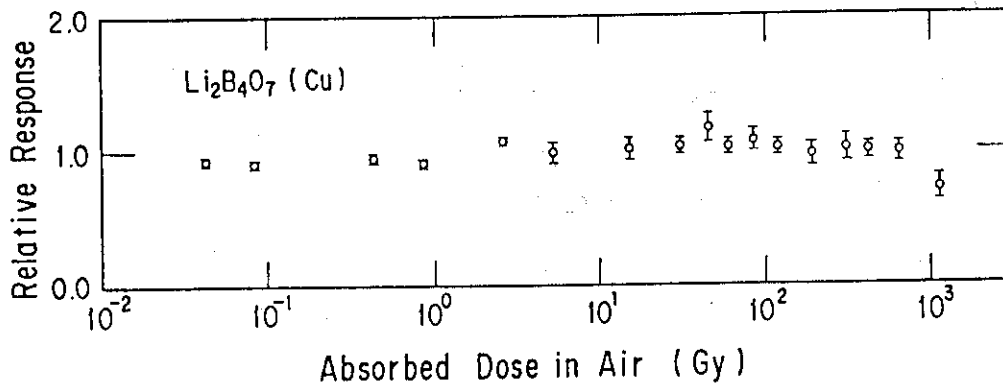


Fig. 14 TL dose response of  $\text{Li}_2\text{B}_4\text{O}_7(\text{Cu})$  to  $^{60}\text{Co}$  gamma-rays. Supralinearity was not observed.

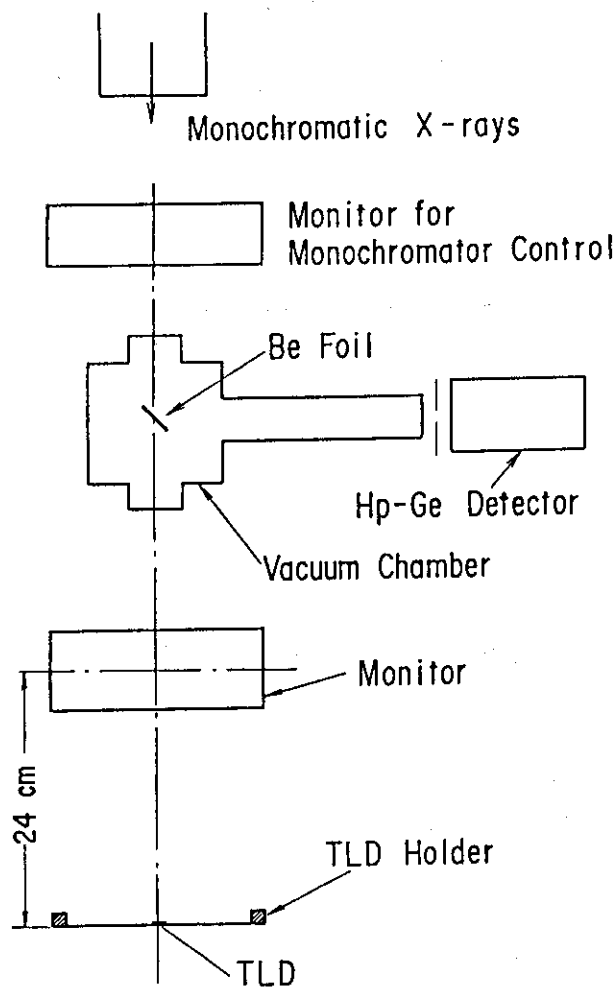


Fig. 15 Experimental configuration of TLD irradiation. The TLD holder was scanned horizontally during irradiation.



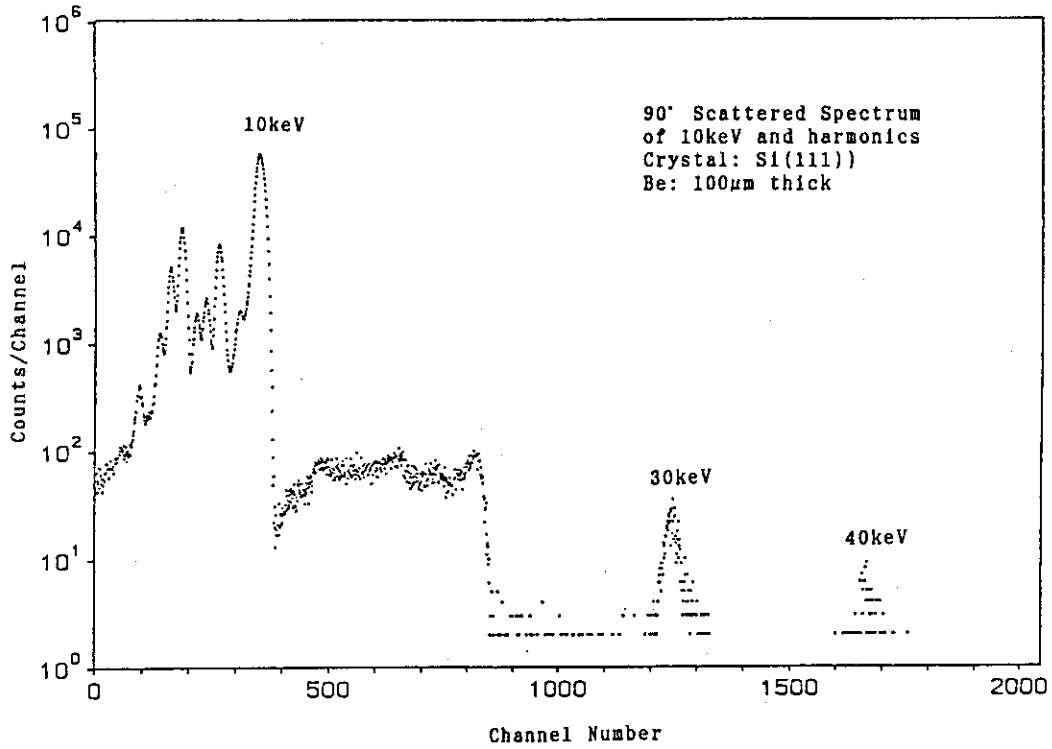


Fig. 16 A 90° scattered spectrum of 10 keV X-ray beam and higher harmonics

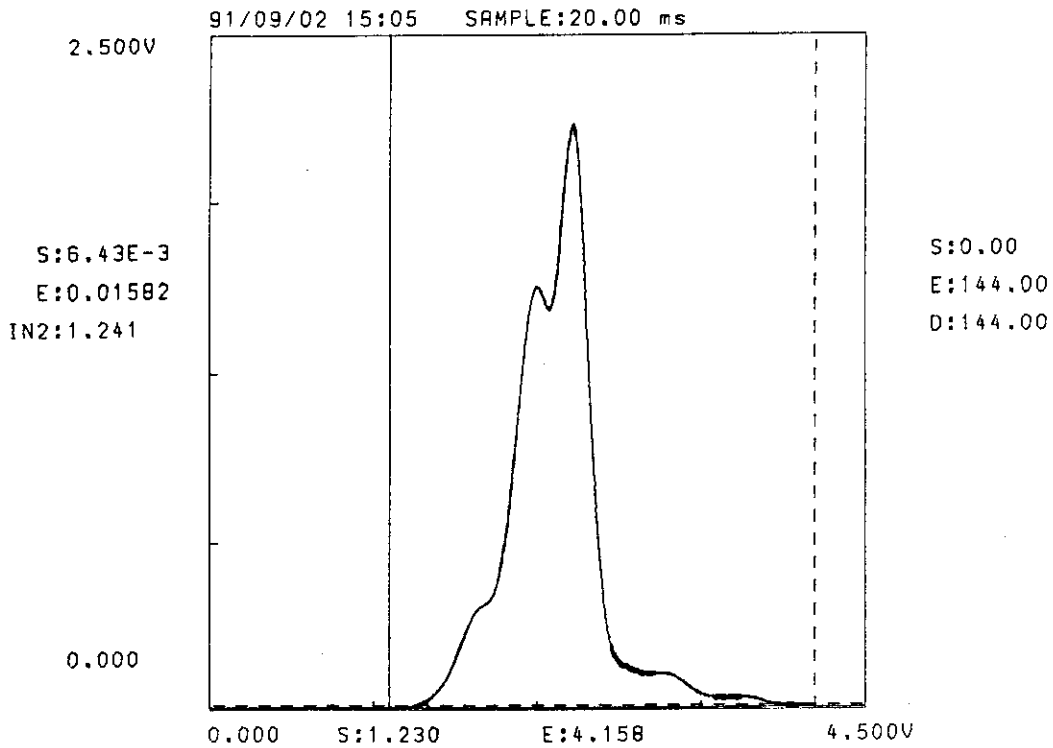


Fig. 17.1 A typical glow curve of LiF to 10 keV X-rays at  $5.14 \times 10^{-1}$  Gy. A heating rate of  $2^\circ\text{C/s}$  was used.

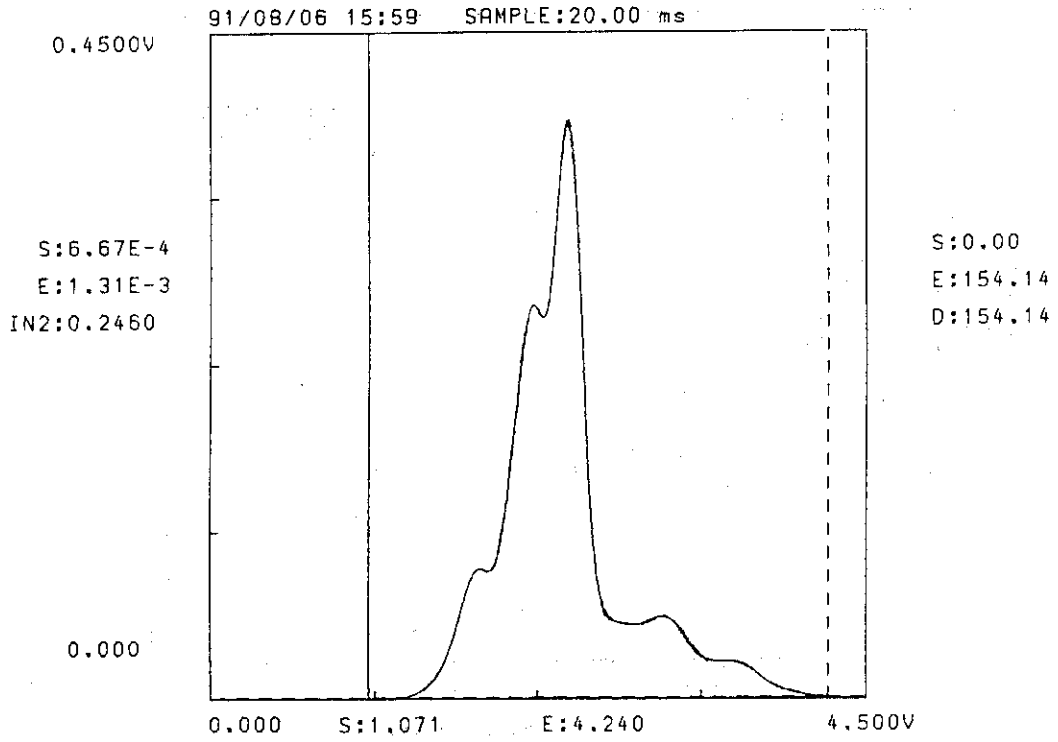


Fig. 17.2 A typical glow curve of LiF to 10 keV X-rays at  $7.29 \times 10^1$  Gy.

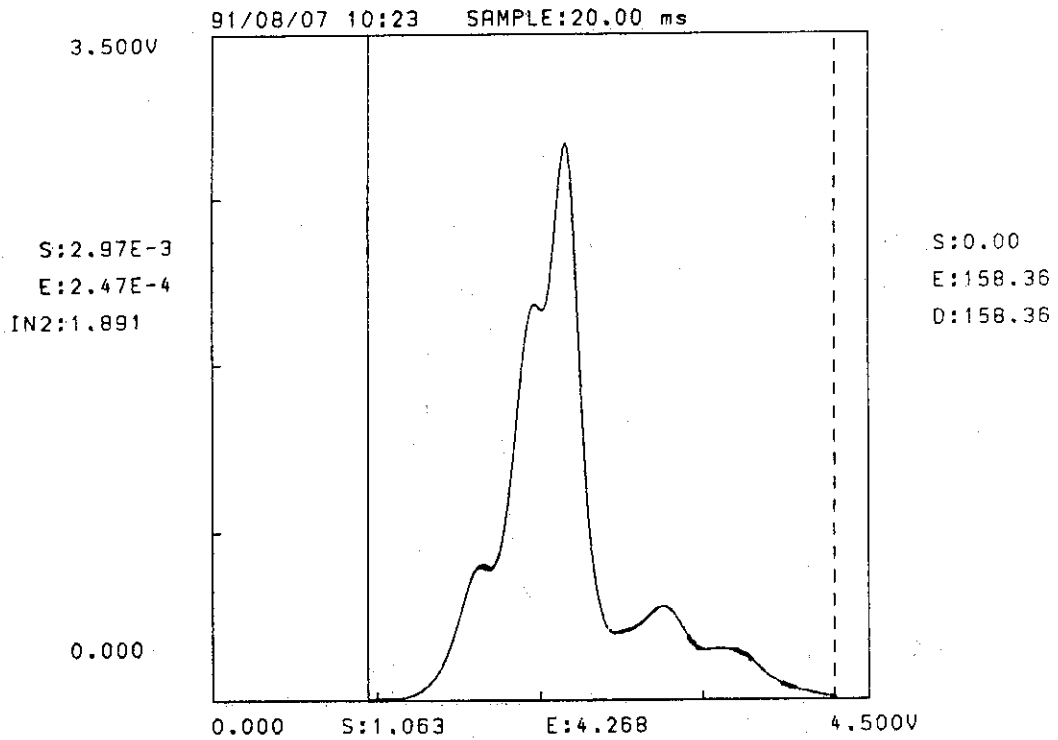


Fig. 17.3 A typical glow curve of LiF to 10 keV X-rays at  $3.54 \times 10^2$  Gy.

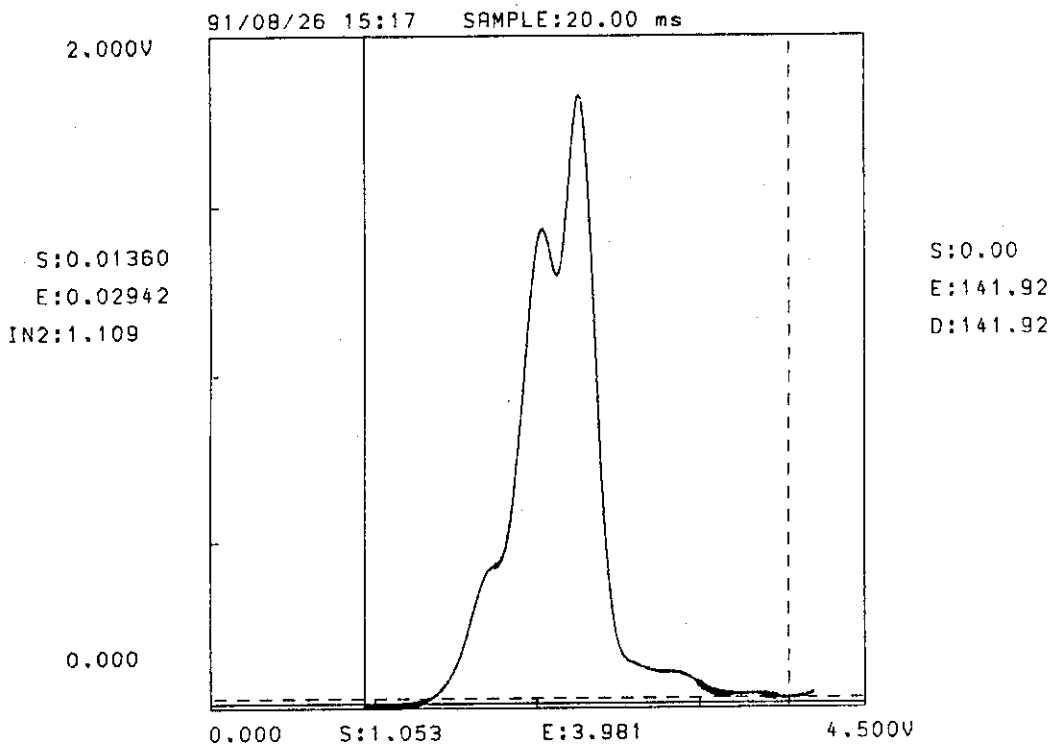


Fig. 17.4 A typical glow curve of LiF to 15 keV X-rays at  $3.84 \times 10^{-1}$  Gy.

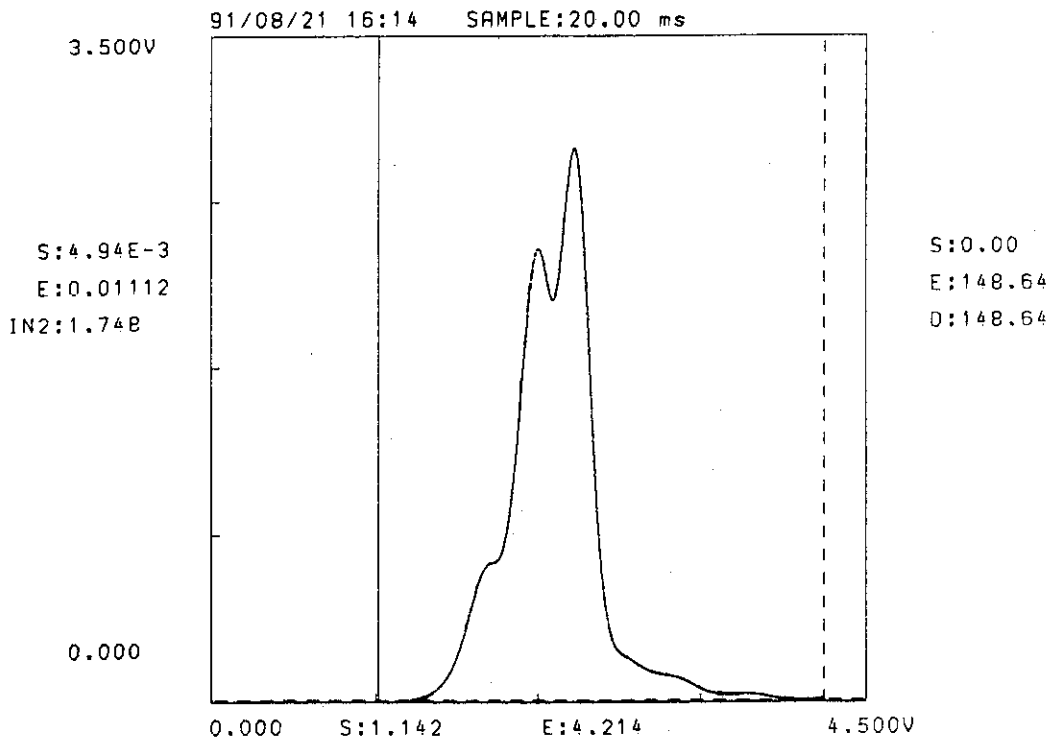


Fig. 17.5 A typical glow curve of LiF to 20 keV X-rays at  $5.17 \times 10^{-1}$  Gy.

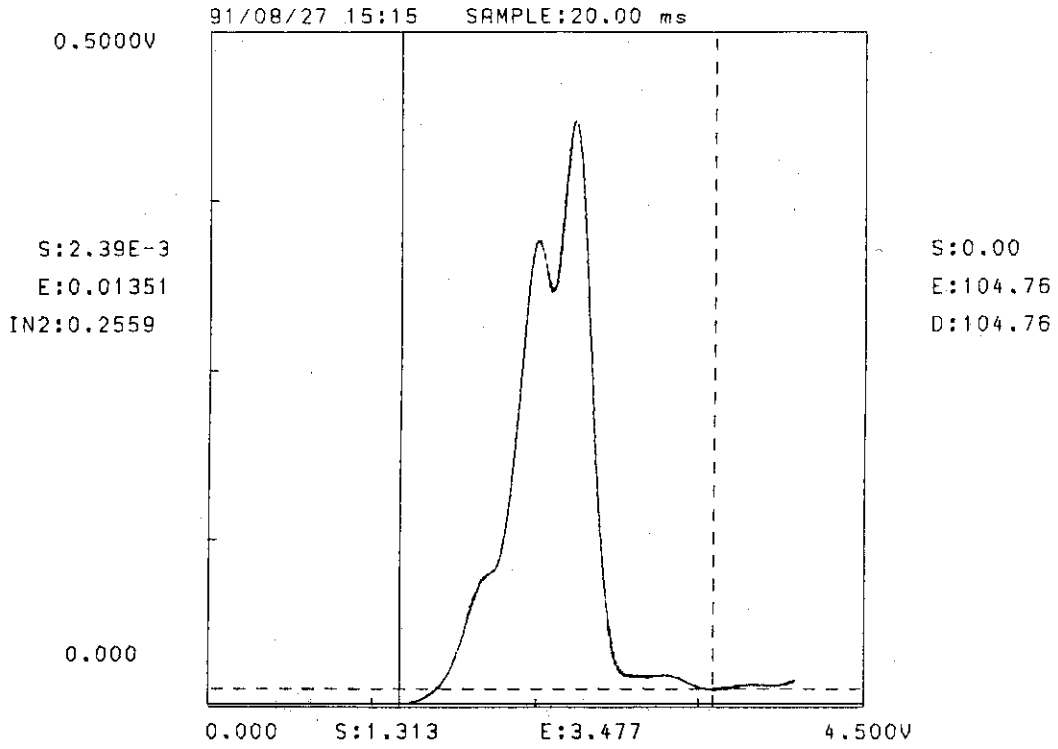


Fig. 17.6 A typical glow curve of LiF to 25 keV X-rays at  $7.85 \times 10^{-2}$  Gy.

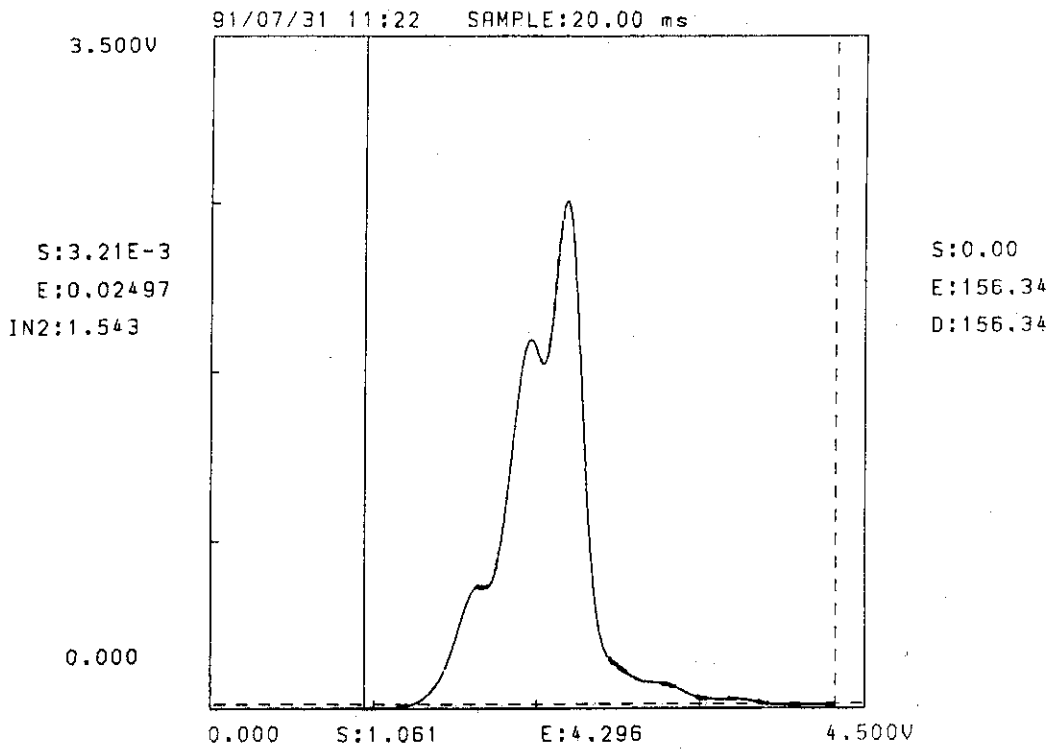


Fig. 17.7 A typical glow curve of LiF to 30 keV X-rays at  $4.65 \times 10^{-1}$  Gy.

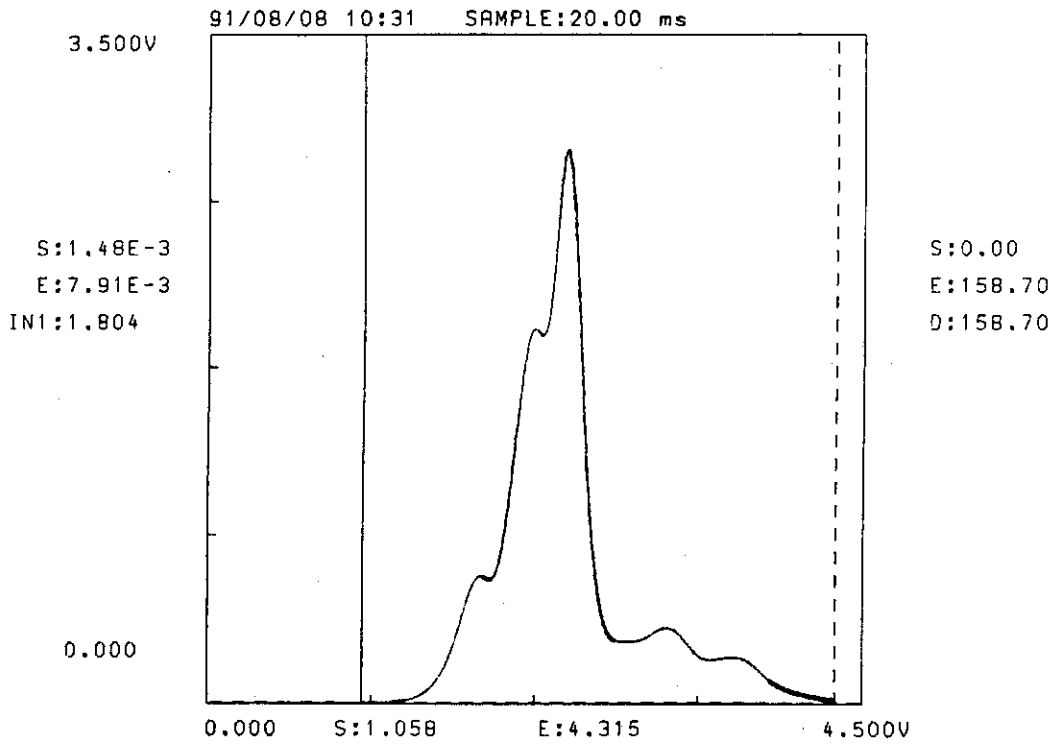


Fig. 17.8 A typical glow curve of LiF to 30 keV X-rays at  $2.61 \times 10^2$  Gy.

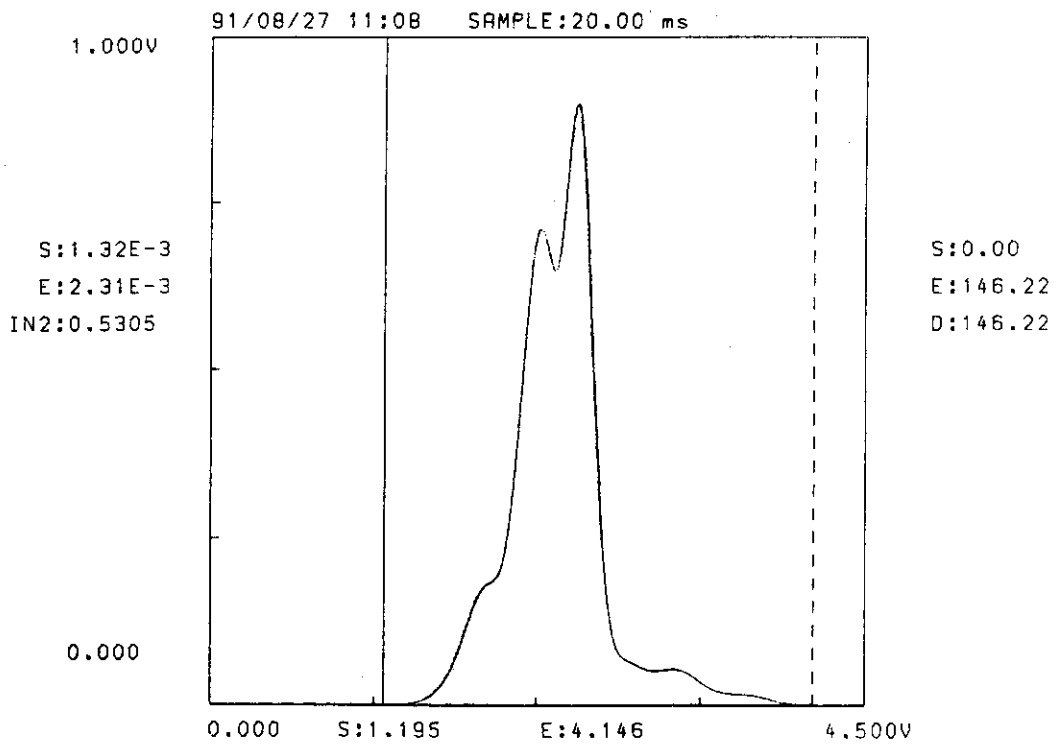


Fig. 17.9 A typical glow curve of LiF to 35 keV X-rays at 1.59 Gy.

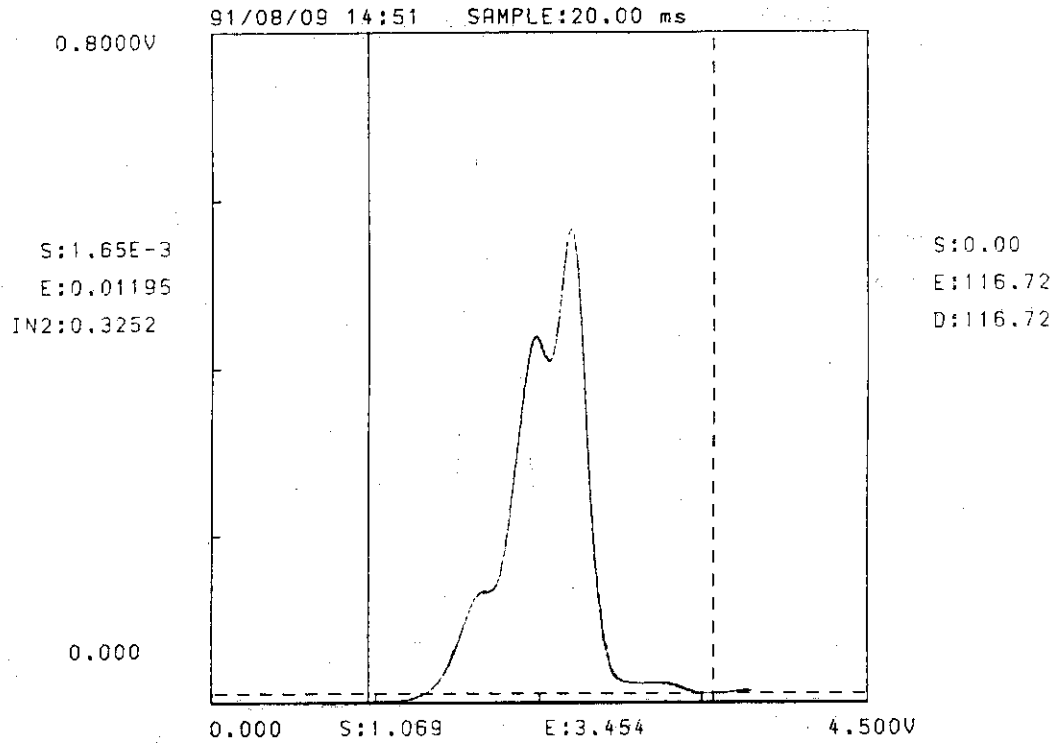


Fig. 17.10 A typical glow curve of LiF to 40 keV X-rays at  $1.02 \times 10^{-1}$  Gy.

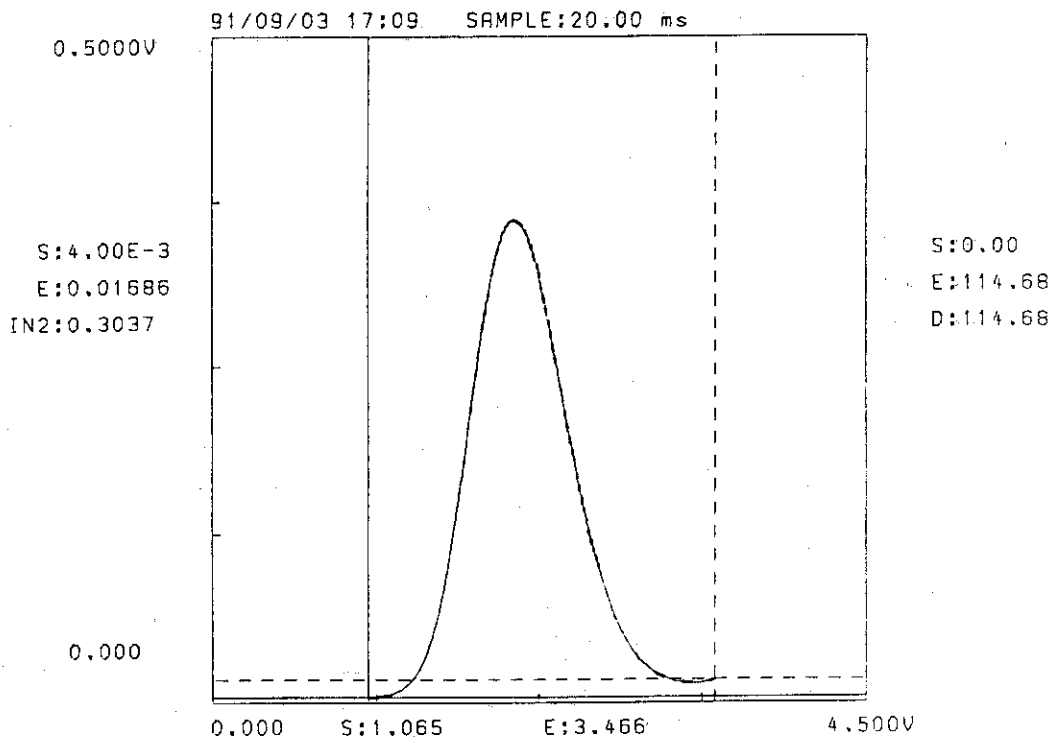


Fig. 18.1 A typical glow curve of  $\text{Li}_2\text{B}_4\text{O}_7(\text{Mn})$  to 10 keV X-rays at 5.14 Gy. A heating rate of  $2^\circ\text{C}/\text{s}$  was used.

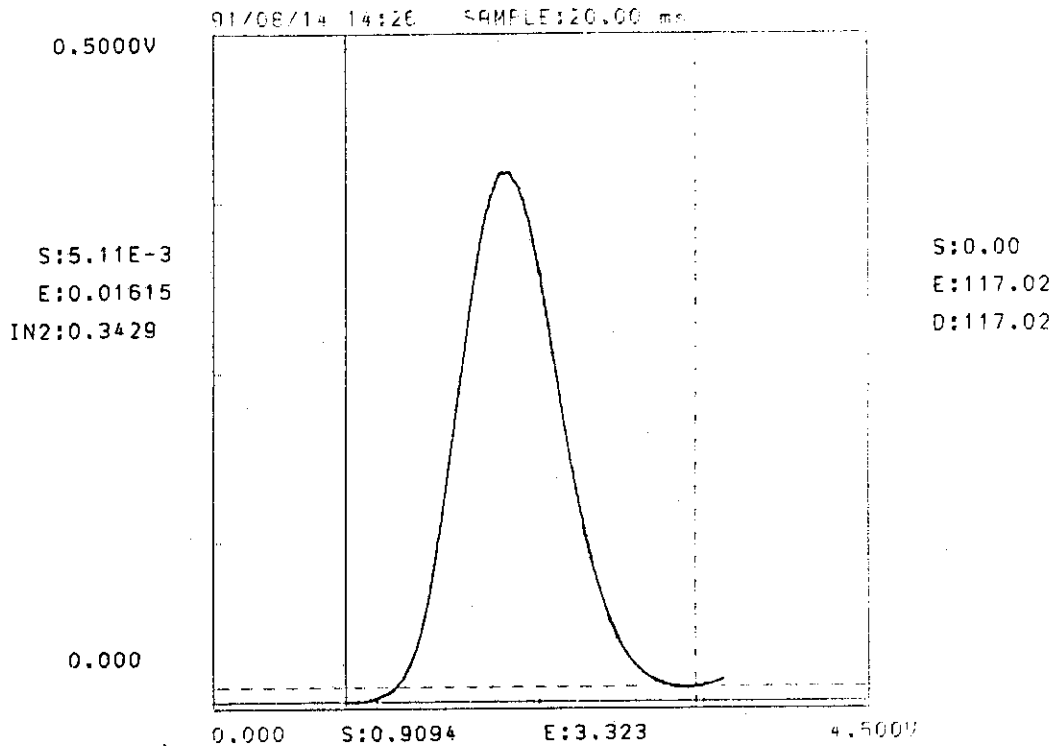


Fig. 18.2 A typical glow curve of  $\text{Li}_2\text{B}_4\text{O}_7(\text{Mn})$  to 15 keV X-rays at 4.37 Gy.

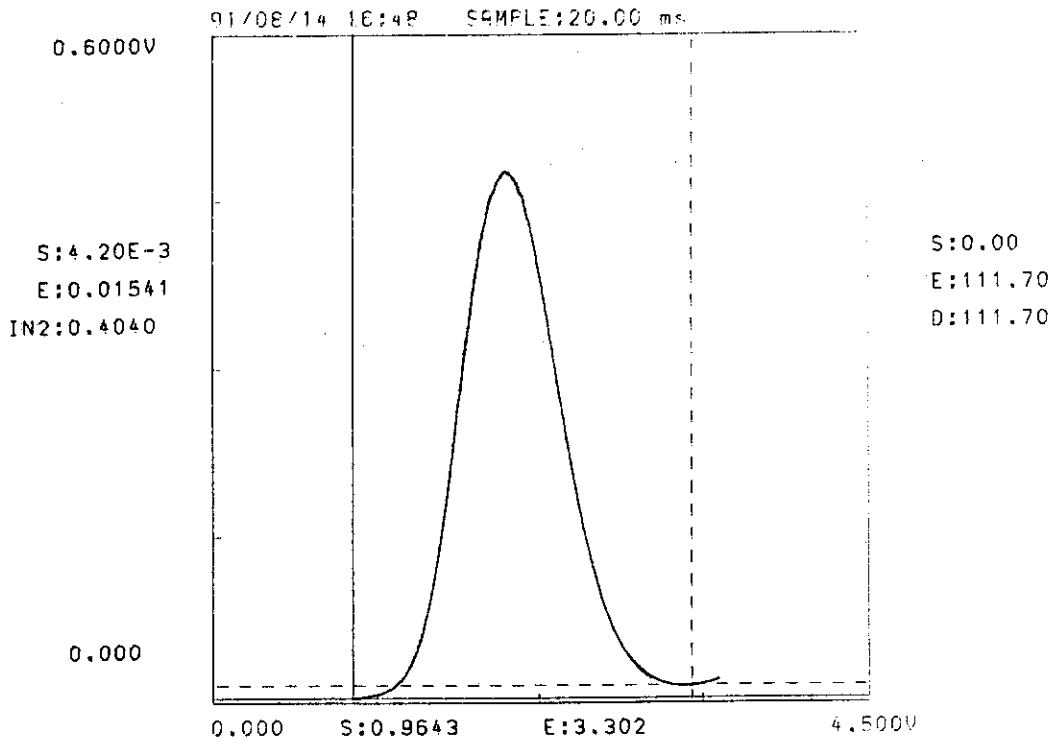


Fig. 18.3 A typical glow curve of  $\text{Li}_2\text{B}_4\text{O}_7(\text{Mn})$  to 20 keV X-rays at 5.01 Gy.

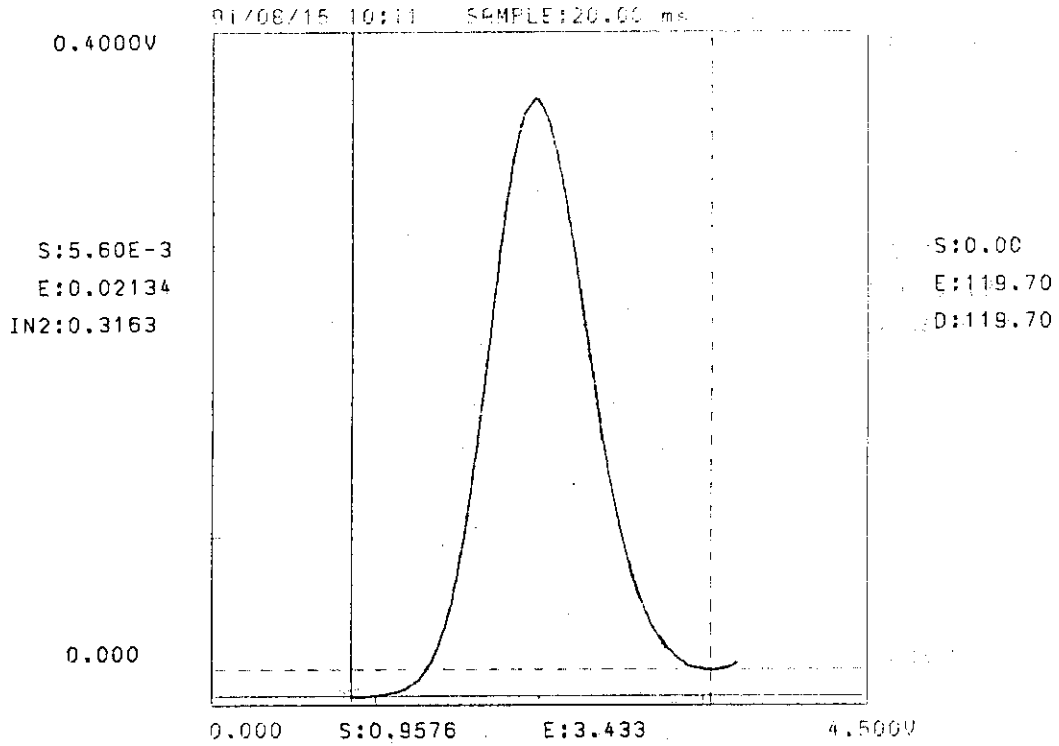


Fig. 18.4 A typical glow curve of  $\text{Li}_2\text{B}_4\text{O}_7(\text{Mn})$  to 25 keV X-rays at 3.75 Gy.

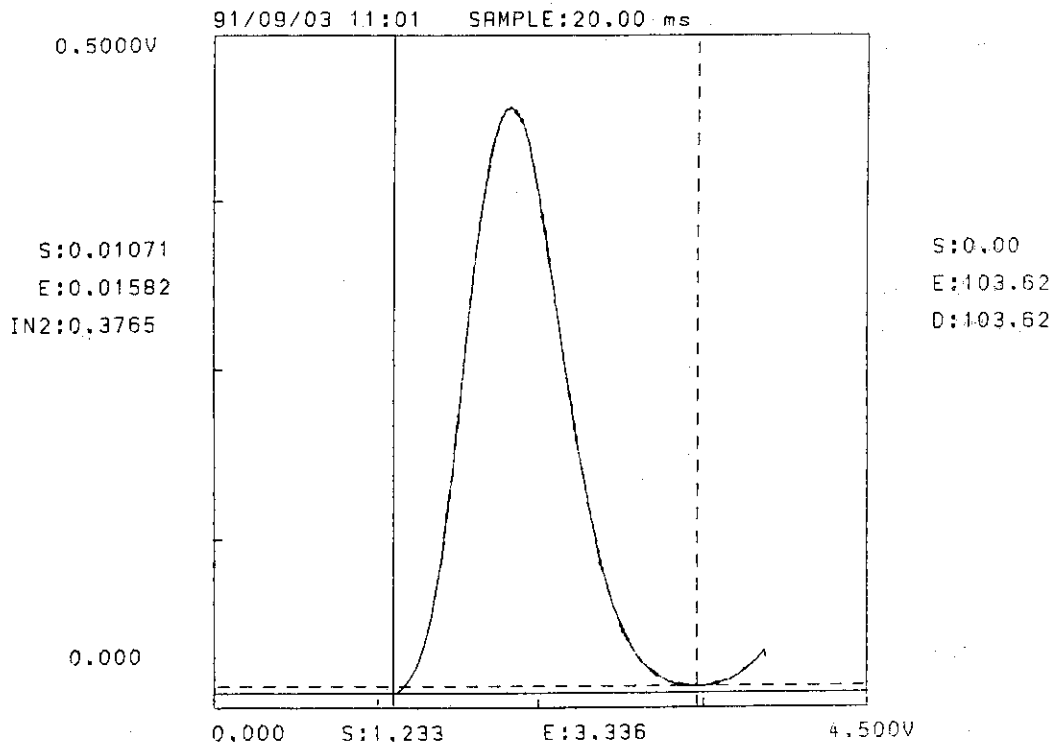


Fig. 18.5 A typical glow curve of  $\text{Li}_2\text{B}_4\text{O}_7(\text{Mn})$  to 30 keV X-rays at 4.70 Gy.



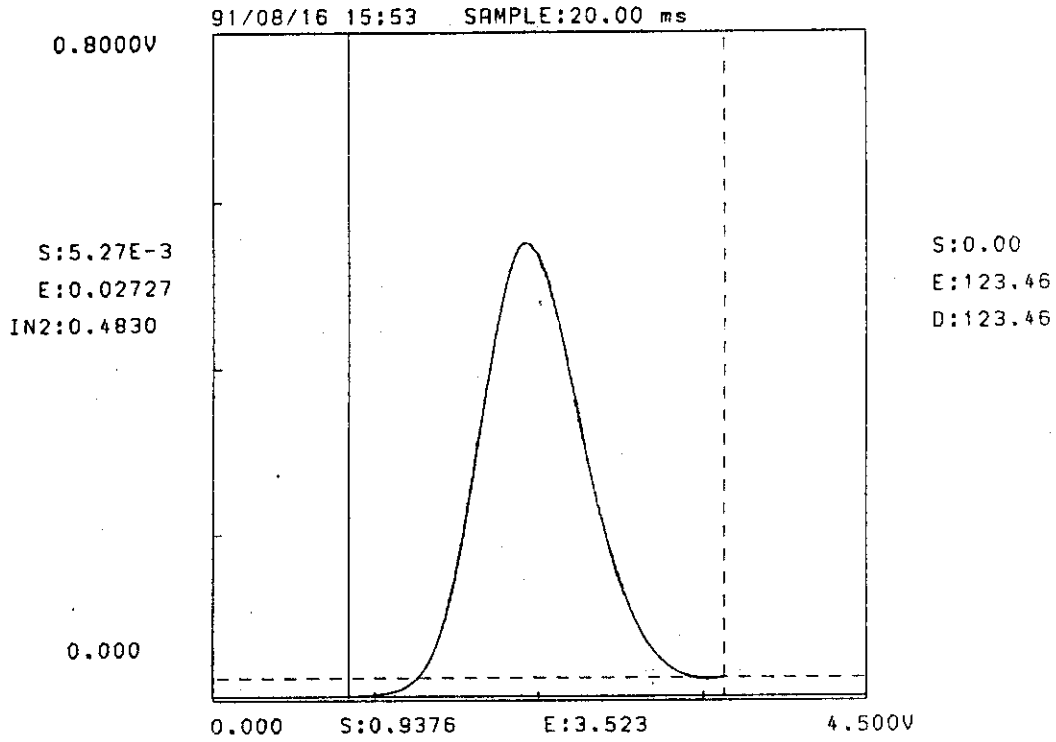


Fig. 18.6 A typical glow curve of  $\text{Li}_2\text{B}_4\text{O}_7(\text{Mn})$  to 35 keV X-rays at 5.55 Gy.

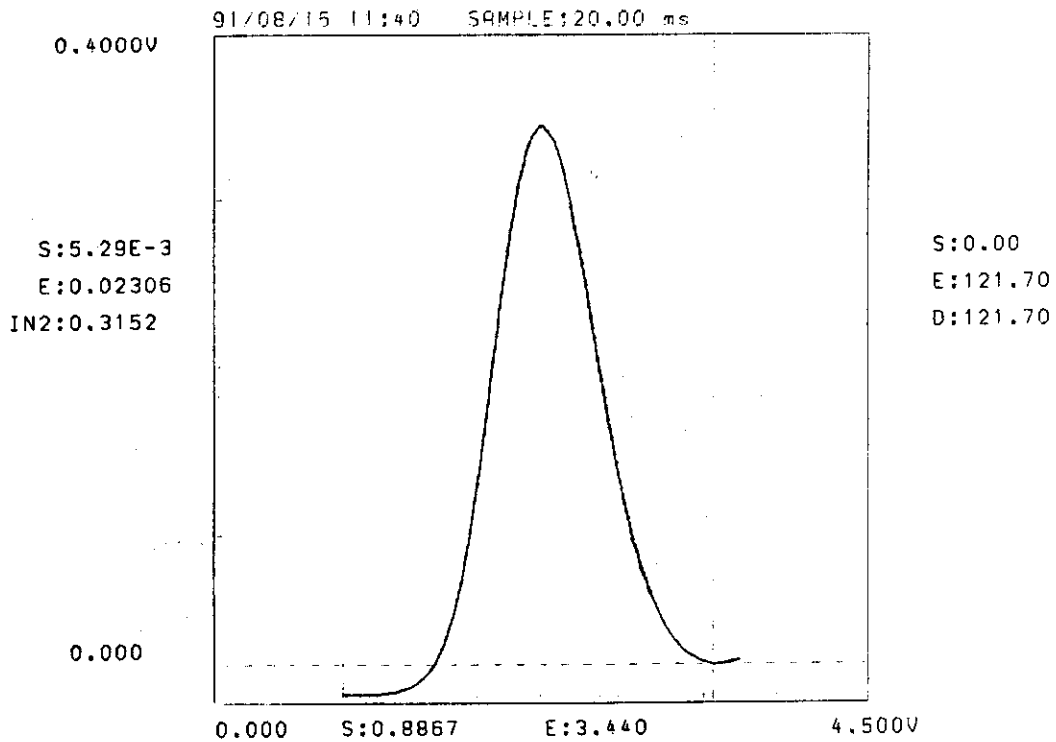


Fig. 18.7 A typical glow curve of  $\text{Li}_2\text{B}_4\text{O}_7(\text{Mn})$  to 40 keV X-rays at 3.59 Gy.

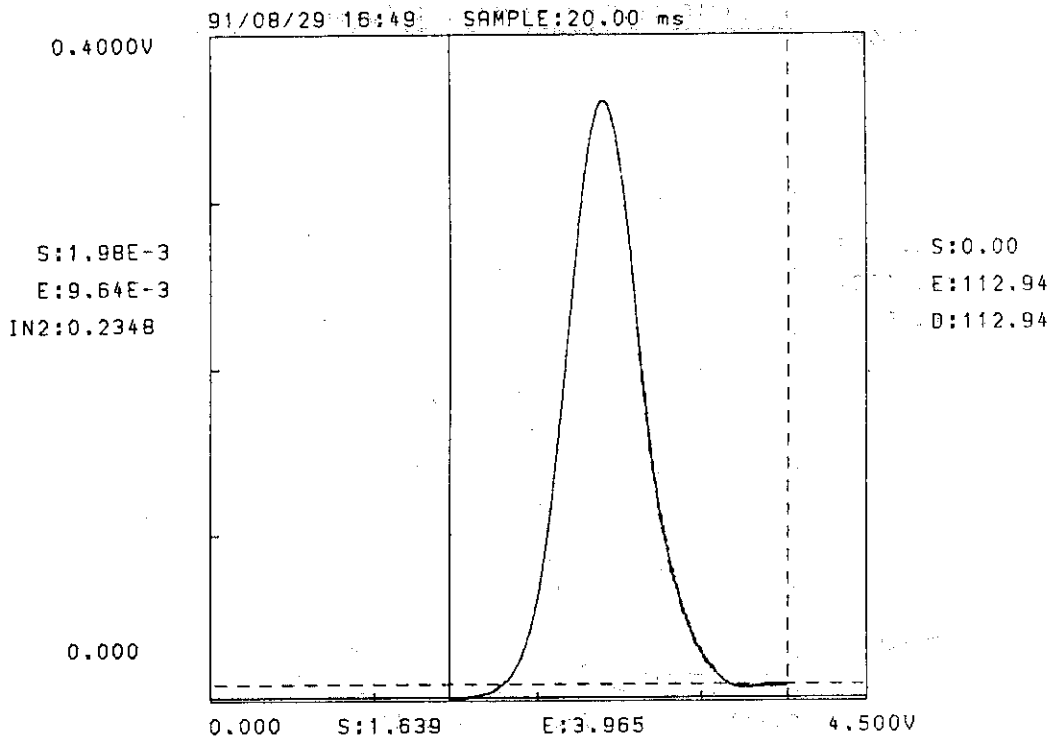


Fig. 19.1 A typical glow curve of  $\text{Li}_2\text{B}_4\text{O}_7(\text{Cu})$  to 10 keV X-rays at 4.88 Gy. A heating rate of  $2^\circ\text{C/s}$  was used.

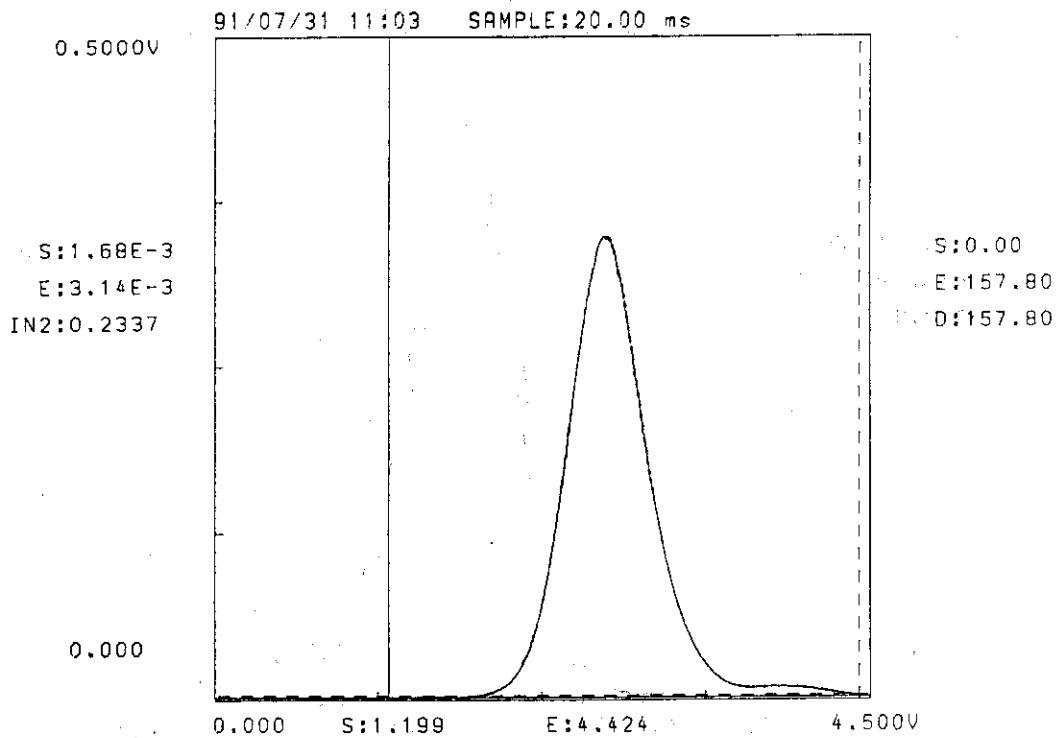


Fig. 19.2 A typical glow curve of  $\text{Li}_2\text{B}_4\text{O}_7(\text{Cu})$  to 15 keV X-rays at 4.17 Gy.

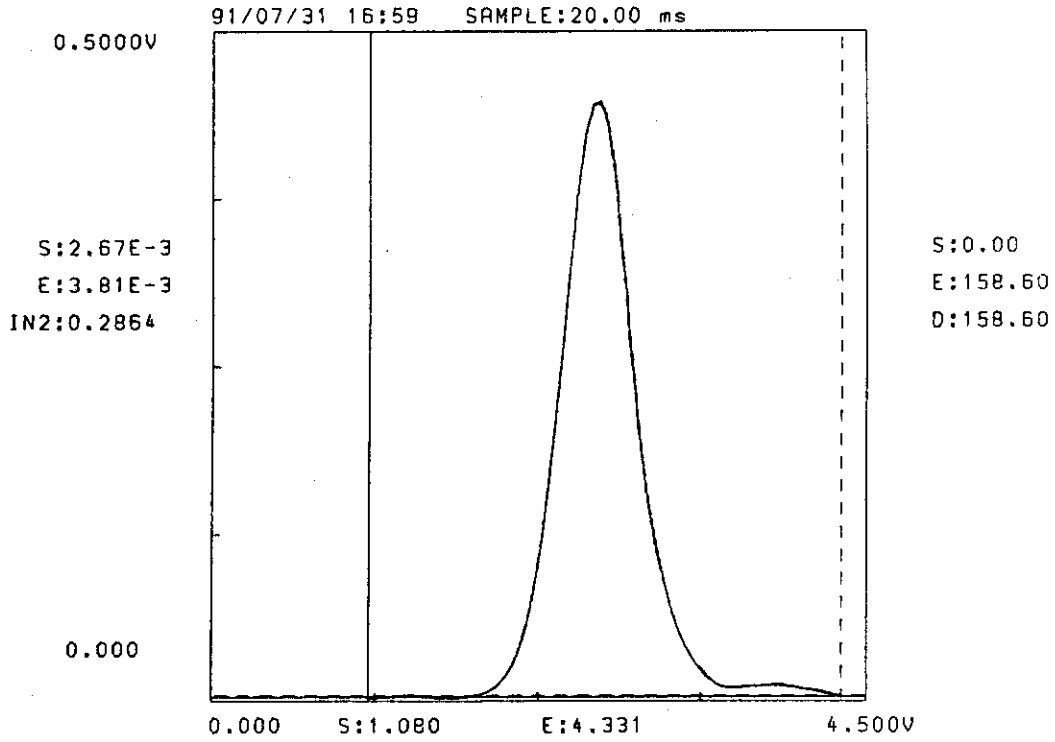


Fig. 19.3 A typical glow curve of  $\text{Li}_2\text{B}_4\text{O}_7(\text{Cu})$  to 20 keV X-rays at 5.16 Gy.

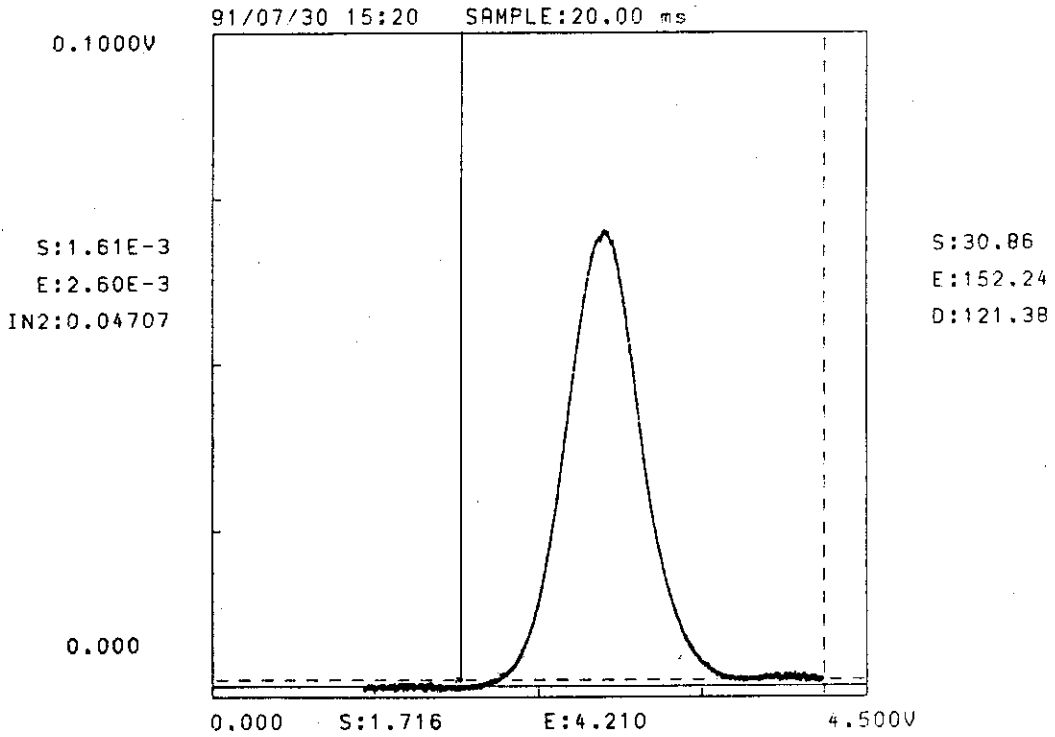


Fig. 19.4 A typical glow curve of  $\text{Li}_2\text{B}_4\text{O}_7(\text{Cu})$  to 25 keV X-rays at 0.834 Gy.

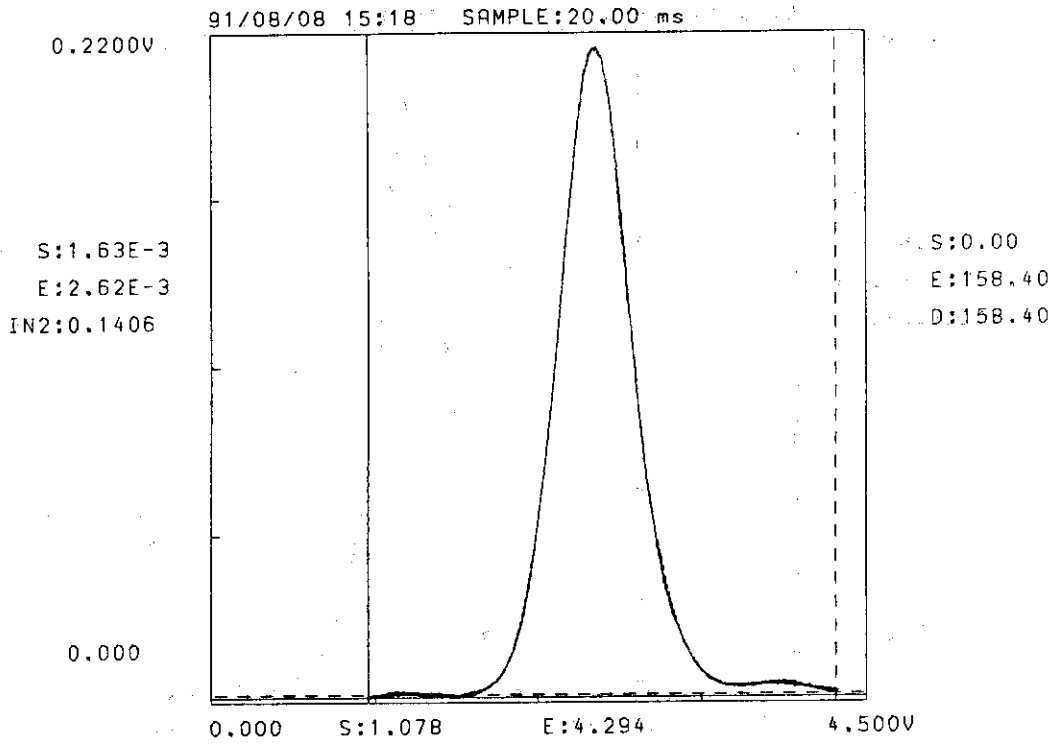


Fig. 19.5 A typical glow curve of  $\text{Li}_2\text{B}_4\text{O}_7(\text{Cu})$  to 30 keV X-rays at 2.08 Gy.

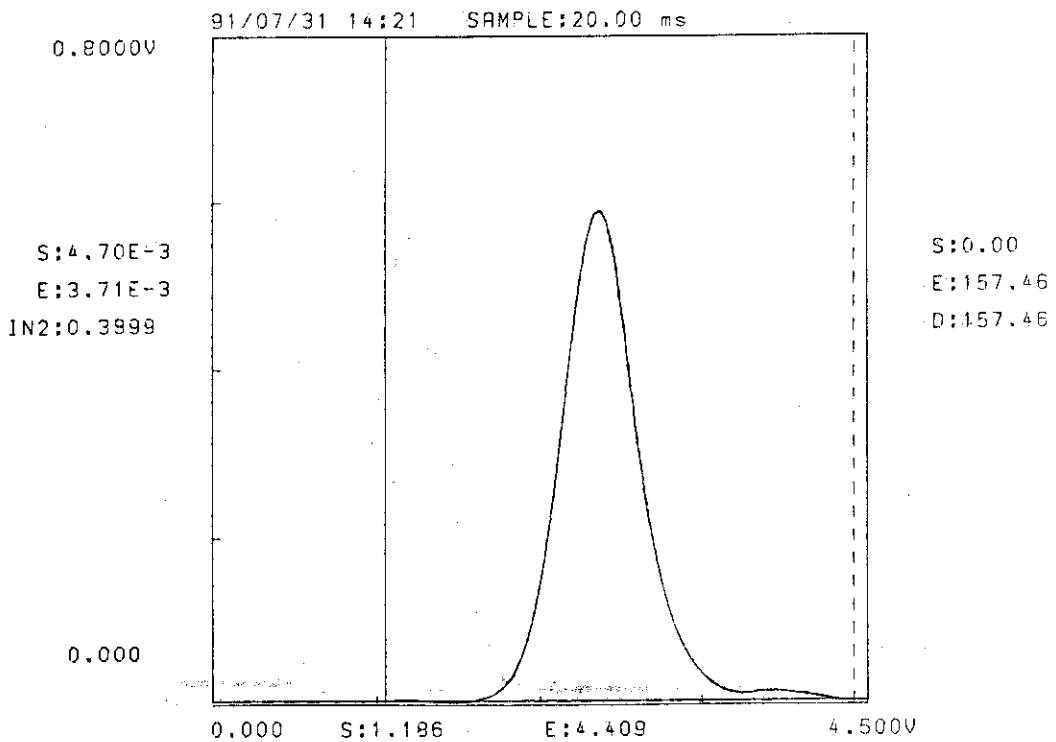


Fig. 19.6 A typical glow curve of  $\text{Li}_2\text{B}_4\text{O}_7(\text{Cu})$  to 35 keV X-rays at 6.03 Gy.

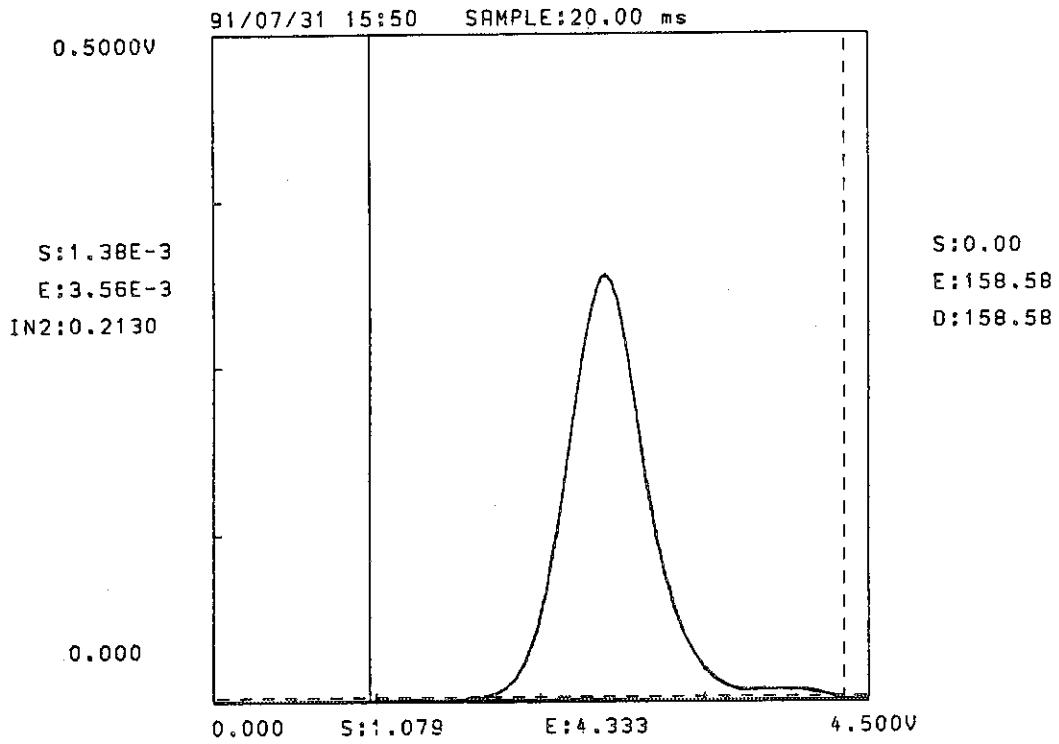


Fig. 19.7 A typical glow curve of  $\text{Li}_2\text{B}_4\text{O}_7(\text{Cu})$  to 40 keV X-rays at 3.73 Gy.

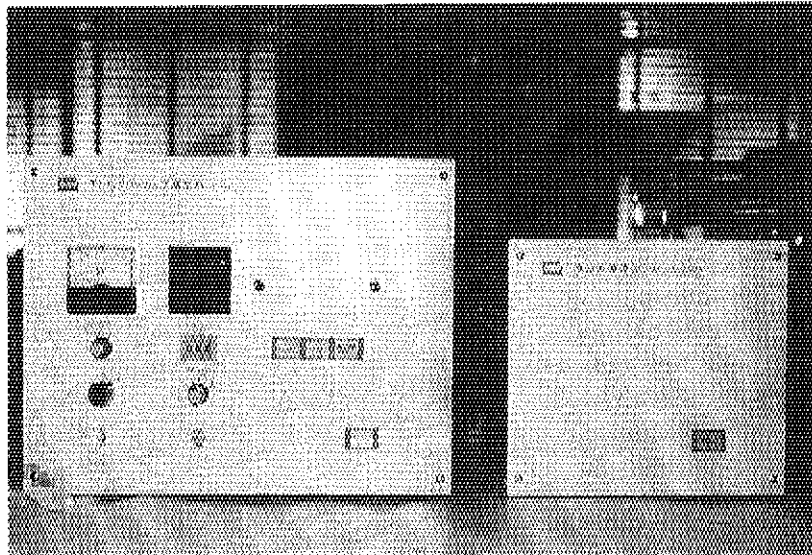


Photo. 1 Front view of the TLD reader system. Left is a TLD reader unit, right is a cooling water unit.